Additive manufacturing of micropatterned functional surfaces: a review

OPEN ACCESS
IOP Publishing | IMMT
International Journal of Extreme Manufacturing
Int. J. Extrem. Manuf. **6** (2024) 042004 (29pp)
https://doi.org/10.1088/2631-7990/ad4240

Topical Review

Additive manufacturing of micropatterned functional surfaces: a review

Aditya Chivate and Chi Zhou*

Department of Industrial and Systems Engineering, University at Buffalo, The State University of New York, Buffalo, NY 14260, United States of America

E-mail: chizhou@buffalo.edu and adityatu@buffalo.edu

Received 8 November 2023, revised 3 February 2024
Accepted for publication 23 April 2024
Published 8 May 2024

Abstract

Over the course of millions of years, nature has evolved to ensure survival and presents us with a myriad of functional surfaces and structures that can boast high efficiency, multifunctionality, and sustainability. What makes these surfaces particularly practical and effective is the intricate micropatterning that enables selective interactions with microstructures. Most of these structures have been realized in the laboratory environment using numerous fabrication techniques by tailoring specific surface properties. Of the available manufacturing methods, additive manufacturing (AM) has created opportunities for fabricating these structures as the complex architectures of the naturally occurring microstructures far exceed the traditional ways. This paper presents a concise overview of the fundamentals of such patterned microstructured surfaces, their fabrication techniques, and diverse applications. A comprehensive evaluation of micro fabrication methods is conducted, delving into their respective strengths and limitations. Greater emphasis is placed on AM processes like inkjet printing and micro digital light projection printing due to the intrinsic advantages of these processes to additively fabricate high resolution structures with high fidelity and precision. The paper explores the various advancements in these processes in relation to their use in microfabrication and also presents the recent trends in applications like the fabrication of microlens arrays, microneedles, and tissue scaffolds.

Keywords: additive manufacturing, micropatterned surfaces, drop-on-demand inkjet, DLP printing

* Author to whom any correspondence should be addressed.

2631-7990/24/042004+29$33.00

1. Introduction

Imagine surfaces, that by design, are crafted to repel water, encourage precise fluid flow, flaunt superhydrophobic, oleophobic, or even omniphobic qualities. Picture surfaces capable of adhering to objects, bonding with flat surfaces, playing with light, or gently piercing the skin without causing discomfort. Visualize dynamic structures capable of generating captivating colors in response to shifting lighting conditions. All of these remarkable attributes can be found in the natural world and have been replicated, at least in laboratory experiments, by manipulating surface microstructures. Microstructures are a common feature in nearly all naturally occurring surfaces, serving a wide array of functions, from enhancing structural integrity to regulating temperature, promoting surface adhesion, achieving hydrophobicity, controlling wetting, enabling self-cleaning, preventing fouling, and even facilitating sensing [1–8]. These surface alterations are prevalent throughout the biological realm and have inspired numerous technological advancements. Many of these intriguing characteristics emerge from surface architectures that exist on a micron scale, well above the molecular level.

Consider the Namib Beetle, commonly found in the arid African deserts, which has evolved with tiny bumps on its back. These bumps allow morning fog to condense and trickle down to the beetle's mouth [9]. Sharks, known for their exceptional swimming abilities, owe part of their prowess to their evolved skin, adorned with micron-sized riblets that reduce drag and promote efficient fluid flow [10, 11]. Rose petals and lotus leaves exemplify natural surfaces that showcase superhydrophobicity, thanks to their hierarchical structures that enable water to glide off effortlessly while capturing surface impurities. This anti-fouling property arises from the millions of tiny cilia-like structures on their surfaces [12–14]. In a similar vein, controlled adhesion might be attainable by studying the microstructures on gecko feet, which could find applications in robotics and gripping technology [12, 15]. Nature has equipped various organisms with ingenious defense and predatory mechanisms, including super-sharp tips with impressive mechanical strength. American porcupines, worker bees, and the notorious Aedes mosquitoes all possess super-sharp microneedle-like structures that enable painless and seamless penetration. The barbed structures on these microneedles offer robust tissue adhesion, aiding some organisms in securing their prey [16]. Nature has honed these structures over millions of years of evolution, resulting in extraordinary complexity and intricacy. Integrating such intricacies into engineered surfaces and structures can yield significant benefits in numerous applications. Biology has consistently favored efficient and energy-conserving solutions, often operating at scales significantly larger than atoms or molecules. Even subtle modifications in architecture can give rise to entirely new properties, and alterations to the surface can introduce exciting new functionalities. Surface modifications and structures with periodicity are natural tendencies, and a bioinspired micropatterning strategy offers inherent advantages over chemical modifications for achieving similar functionality. By using fewer materials and relying less on chemical alterations, these micropatterned structures offer enhanced stability, resilience, and superior resource efficiency. Beyond biologically inspired structures, numerous micropatterned surfaces have demonstrated promising applications across various fields. Nature's inspiration, such as compound eyes seen in many anthropoids, has led engineers to fabricate diverse microdome arrays that extend well beyond optical applications. These arrays offer versatility in addressing a range of needs. Furthermore, microneedle arrays (MNA), designed with various considerations, have found applications beyond their initial use in epidermal patches. These arrays have proven valuable in drug delivery systems, showcasing the adaptability and impact of micropatterned surfaces in advancing innovative solutions across different domains.

What nature has done over millions of years as a result of natural selection is difficult to mimic with traditional manufacturing techniques. Numerous techniques have been proposed to investigate and achieve ultraprecision manufacturing processes, such as milling, turning, three-dimensional printing, lithography, and some other chemical manipulation techniques [17, 18]. Micro and nano imprinting is a widely used technique for fabricating uniform and repetitive tiny features such as micro lenses and micro needles [19]. Chemical etching techniques are widely used for achieving precise control over the mold. Diamond, silicon wafers, ITO, etc, are a general choice for this process due to their directional properties [20, 21]. There exist numerous other techniques as well, including but not limited to hot embossing, photoresist reflow, femtosecond laser direct writing, ink jetting, digital light projection (DLP) printing, electrohydrodynamic jetting, and photolithography [20, 22–25]. Nature uses additive approaches to build these structures, so it only makes sense to use additive techniques for fabrication. 3D printing is a disrupting manufacturing technique that is changing the way we fabricate intricate objects. Recent advancements have paved the way for fabricating micron-scaled objects as evident from figure 1. Numerous additive techniques exist that can add material layer by layer to fabricate complex geometries and micro-patterned surfaces.

However, a systematic review of fabrication techniques for patterned microstructure arrays is lacking. Therefore, we have presented a comprehensive review of the recent advancements in microstructure arrays, their fabrication techniques, and applications. Section 1 introduces different fabrication methods for patterned microstructure arrays. More emphasis is placed on additive techniques for fabrication due to their versatility and flexibility. In section 2, inkjet printing as a potential fabrication option has been presented. The jetting process, droplet formation, material properties, and applications are briefly detailed. Section 3 examines microSLA printing as a viable alternative for microfabricating patterned surfaces. Lastly, we summarize the current advances and the challenges faced in fabrication and point out the future possibilities of microstructure fabrication technology.

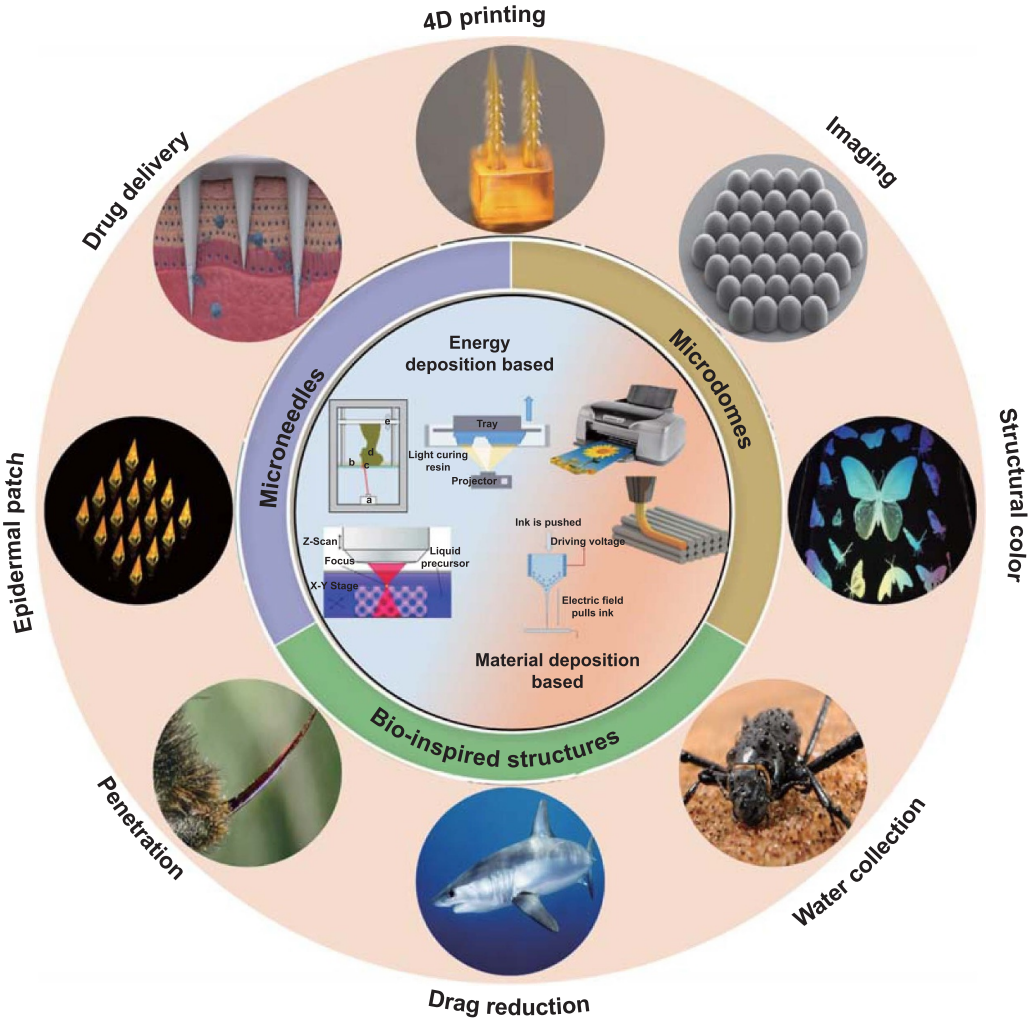

Figure 1. The paradigm of surface micropatterning. A wealth of surface functions created by micropatterning: controlled interaction with other solids, liquids, and soft matter such as skin and tissue.

2. Overview of microfabrication techniques

According to the working principle, the fabrication techniques can be broadly classified into two categories: direct methods and indirect methods. Direct methods refer to techniques that do not require any masks or molds. It does not create any scaffolds to fabricate the microfeatures. Hot embossing, inkjet printing, DLP printing, EHD printing, laser-based fabrication, and self-assembly fall under this umbrella. Indirect methods use multi-step processes to realize the required structure. It utilizes multiple physical masks or chemical processes to first create a negative profile, which then acts as a mold. Soft-lithography and etching are the most commonly used indirect fabrication techniques. In table 1, we summarize the advantages, disadvantages, and resolution of different fabrication processes.

Amongst the various techniques discussed above, each method presents us with a certain set of advantages and limitations. The choice of these methods depends on the resource availability, material compatibility, and the intended applications. These techniques can be broadly classified into direct and indirect methods. Direct fabrication involves the creation of microstructures directly on the target surface, while indirect methods entail the production of microstructures on a separate substrate and subsequent transfer to the desired surface. Indirect methods consist of techniques like etching, molding, and lithography and are immensely popular in the current microfabrication industry due to the long history and process optimization. For instance, techniques like lithography are especially popular in microchip manufacturing, offering extremely high resolution and compatibility with the commonly used materials in microscale manufacturing. However, they are painstakingly slow and require very high process control to achieve high resolution. Etching techniques have long been favored in wafer fabrication due to their simplicity, fabrication speeds, scalability, and extremely high resolution [68]. Despite the advantages, they are burdened with high setup costs, generation of toxic byproducts, lack of sustainability, and limited flexibility. Microscale molding is also a popular choice, particularly for microfluidic fabrication, although the initial mold production costs and the inherent resin-flow dynamics at

Table 1. Different microfabrication techniques with their advantages, disadvantages, and resolution.

Fabrication method			Advantages	Disadvantages	Resolution	References
Direct methods	Embossing	Hot embossing	Straight forward, time efficient, cost effective, high aspect ratio fabrication, compatible with polymer substrate	Difficult to customize, challenging to manufacture overhangs, risk of damage during demolding, overly dependent on template quality, degradation over time, high temperature required	Resolution: 1 μm Aspect Ratio: 10	[23, 26–30]
	3D Printing	Inkjet printing	Customizable, high accuracy, no material wastage, non-contact process, wide variety of substrates, better for mass production, high conformability	Limited material availability, uncertainty in the printing, difficulty in geometry control, prone to nozzle clogging	Resolution: 10–20 μm Aspect ratio: 50:1	[30–36]
		EHD printing	Very high resolution, scalable, 3D printing ability, low setup cost, high substrate compatible, multi-nozzle printing possible	Necessity of conductive substrate, nozzle clogging, fragile hardware, high variability with changes in the applied field	Resolution: 500 nm Aspect ratio: 8:1	[36–40]
		Aerosol jetting	Scalable, high resolution, maskless and non-contact, conformal printing, substrates versatility	Limited material availability, substrate surface preparation desired, less reliable at higher resolution, expensive initial setup	Resolution: 10 μm Aspect ratio: 10–20	[41–43]
		DLP printing	Low cost, high throughput, non-contact process, high resolution, substrates and materials versatility	Staircase pattern in prints, proximity issues, uneven light intensity.	Resolution: $<$5 μm	[6, 44–49]
		2-Photon polymerization	Extremely high resolution, high accuracy, high repeatability, versatile process	High equipment cost, very slow process	Resolution:$<$ 100 nm Aspect ratio: 40	[50–53]
	Others	Self-assembly	Very high surface smoothness, high uniformity, simple process	Difficult to integrate in all systems	Aspect ratio: 10	[54–56]
		Thermal reflow	Simple, low cost	Limited control in z-direction, require mask	Resolution: $<$50 μm Aspect ratio: $<$1	[54, 57–60]
		Ultraprecision micromachining	High surface accuracy, high precision	Low efficiency	Resolution: $<$ 1 μm	[61]
Indirect methods	Lithography	Soft lithography	Low cost, very high resolution	Diffusion from ink can lower resolution, prone to degradation	Resolution: 30 nm–100 nm Aspect ratio: $\sim$2	[62, 63]
	Etching	Wet etching	Simple, fast, highly selective, high throughput, low cost	Toxic byproducts, require cleanroom, poor process control, low precision	Resolution: $>$2 μm	[64, 65]
		Dry etching	High resolution	High cost, low speed, complex process	Resolution: $>$1 μm	[64, 65]
	Molding	Injection molding	Faster process, low cost, precise	Challenging mold preparation, stringent flow control requirement, high mold costs	Resolution: $<$1 μm	[66, 67]

the scale make its realization impractical where flexibility is paramount [69].

Direct methods involve AM, chemical manufacturing, embossing, machining, and others. Hot embossing stands out as a popular direct fabrication method offering high resolution, fast production speeds, and high aspect ratio printing with the ability to use polymer substrates. However, it struggles to customize and build complex structures consisting of overhanging features. Thermal reflow, another heat-based direct microfabrication technique, is capable of achieving sub-micron to a few microns' resolution. The process involves heating of thermally sensitive material to achieve controlled flow, enabling the formation of microstructures. It is advantageous for its simplicity and compatibility with various materials but demands precise temperature control and may have potential material compatibility issues. Certain materials showcase a remarkable ability to self-assemble in ordered structures, offering a scalable and cost-effective direct microfabrication approach. While this approach has been successfully applied for large-scale micropattern fabrication, its applicability remains limited to a select few materials and specific applications, rendering it a niche approach. Ultraprecision micromachining is another niche, high-precision manufacturing method capable of achieving sub-micron accuracy, and providing excellent surface finish and intricate structures. However, it often requires specialized equipment and longer processing times, making it unsuitable for a wide variety of applications.

In nature, the processes of evolution have honed additive techniques over millions of years, giving rise to the extraordinary structures that surround us. These microfeatures generally span from a few microns to a few millimeters. For instance, microneedles typically have a height of a few hundred microns with a tip diameter in the range of a few tens of microns. Likewise, the dimensions of microlenses vary based on the application, ranging from a few tens of microns for applications like structural color to a few millimeters for imaging purposes. Biomedical applications often constrain feature sizes based on cell dimensions. AM offers a solution to overcome most of the discussed limitations while falling under the umbrella of direct manufacturing. It is only logical, then, to leverage these additive methods to engineer the precise microstructures that we aspire to create. As illustrated in table 1, AM techniques find applications in both direct and indirect methods, opening up a world of possibilities for fabricating microscale patterns.

These techniques can be broadly categorized into two primary groups based on their underlying mechanisms: material deposition-based and energy deposition-based methods. Within the realm of energy deposition-based methods, light-based methods have gained popularity, particularly in microfabrication, as they operate on the principal of photon-driven material polymerization and can precisely control the input energy and consequently the feature size. Material deposition-based processes function by meticulously depositing controlled quantities of materials at specific locations. Techniques in this category include fused deposition modeling, binder jetting, wire arc additive manufacturing (AM), direct ink writing, and liquid droplet deposition techniques. Liquid droplet deposition methods, such as inkjet printing, electrohydrodynamic printing, and aerosol jet printing, are particularly favored for depositing controlled amounts of material in the form of minuscule picolitre droplets at specific locations. Among these, drop-on-demand inkjet printing stands out for its versatility and robustness, accommodating a wide variety of functional materials. Conversely, light-based techniques harness specific wavelengths of light to solidify photosensitive resins into desired shapes. Within this category, we encounter various stereolithographic processes, including two-photon photopolymerization, DLP printing, and laser-based 3D printing, each of which possesses distinctive features and applications. Two-photon photopolymerization can achieve sub-micron resolution but is slow with low throughput. Laser scanning-based processes are relatively faster, but their effectiveness in realizing arrays of micropatterned structures is limited by the laser spot size and scanning speed. Among light-based techniques, DLP stands out for its ability to parallelly print the entire micropattern array by projecting large images. DLP systems also offer excellent tunability through tunable optics, gaining traction in the microfabrication field due to their versatility and efficiency.

By exploring the possibilities within these AM methods, we are equipped with a versatile toolkit for generating microstructures that hold immense promise across a spectrum of fields, from materials science to biotechnology and beyond. In the following sections, we will briefly discuss the current progress in deposition-based as well as light-based techniques for producing functional surfaces with microstructures.

3. Material deposition-based micromanufacturing techniques

Material deposition techniques are gaining popularity in the realms of microfabrication due to their ability to precisely deposit controlled amounts of materials. As the amount of material and the placement can be accurately controlled, these techniques have found applications in micro-optics, electronics, and biomedical fields [31, 32, 70–72]. The deposition-based techniques can be further classified based on the type of material being deposited and the deposition mechanism. Techniques like fused deposition modeling and direct ink writing deposit semi-solid paste-like materials through an extruder nozzle loaded on a gantry system. Due to the inherent nature of the material used in these systems, they can only achieve a certain resolution, which makes them ineffective for microfabrication applications. Droplet deposition techniques, on the other hand, use liquid materials and deposit-controlled amounts of these liquid inks in the form of tiny droplets or liquid streams. Due to the ability of these techniques to deposit picolitre volumes of the liquid material, they become an obvious choice for microfabrication.

The liquid deposition techniques can be further divided into three main categories based on the material ejection mechanism. Aerosol jetting is an advanced AM technique that precisely deposits tiny droplets of material onto surfaces, enabling the creation of intricate three-dimensional structures with high

resolution and fine detail. It involves atomizing a liquid material into tiny droplets suspended in gas, which are then deposited on the substrate in a layer-by-layer fashion. Fluid dynamics of gas flow is utilized to atomize and transport liquid material as aerosol droplets, which solidify upon the impact with the substrate and build complex 3D structures influenced by the material properties and substrate interactions. Owing to its <10 μm resolution, it is particularly valuable for applications requiring microscale features and complex geometries. It distinguishes itself by allowing non-contact printing on conformal surfaces, making it versatile for numerous applications like micro-optics, waveguides, conformal antennas, and biosensors [41, 43]. However, it does have some drawbacks, such as slower printing speeds compared to other methods, limited build volume for larger objects, lesser reliability at higher resolutions, the necessity for specialized equipment, and the potential cost implications associated with specialized inks. Due to these limitations, the need for highly specialized inks and slower printing speeds has constrained its involvement in the mass production of microstructured surfaces and deemed it a niche fabrication process. Electrohydrodynamic jetting is another popular liquid material jetting technique that employs electrostatic force to precisely deposit conductive liquid inks onto a charged substrate. A voltage is applied to the ink, which creates an electric field that induces surface charges on the ink droplets, causing them to form a fine, controllable jet. The jet is directed towards a substrate, where the ink solidifies upon deposition, layer by layer, forming a three-dimensional structure. This process is highly controlled and can achieve high-resolution prints, finding applications in electronics and microfluidics [36, 73, 74]. However, it has limitations regarding material compatibility, printing speed, equipment complexity, and scaling for larger objects. The inherent precise nature of the process makes it a slow process, thus making it challenging to scale, and the requirement for material charging makes the use of many materials infeasible.

Inkjet printing, another one of the liquid material jetting techniques, is highly regarded for its versatility and widespread use. Its simplicity, scalability, and compatibility with a wide range of materials have contributed to its prominence. Beyond its traditional role in office applications like paper printing, inkjet technology has made significant inroads into new domains such as printing electronics, optics, and micro-electro-mechanical systems (MEMS) devices. Inkjet printing boasts advantages, including high throughput, fast printing rates, flexibility, and cost-effectiveness, all while minimizing material wastage [75]. It relies on a limited number of functional materials, ranging from simple polymer solutions to complex nanoparticles. This section delves into the intricacies of the inkjet process, elucidating its various steps, optimization techniques, and multifaceted applications across different industries.

3.1. Fundamentals of inkjet printing

Inkjet printing is a non-contact process which is ideal for the immobilization of functional materials without the risk of cross-contamination. It delivers picolitre droplets in reproducible volumes in response to the input signal. This digital control allows each pattern printed by the same machine to be just as readily different from each other as it can be the same. This technology that was commercially made available in the 1970's was primarily used for printing low-resolution texts has matured over the years and now can print very high-resolution patterns with high accuracy and repeatability.

Inkjet printing can be broadly categorized as continuous ink jetting (CIJ) and drop-on-demand inkjet printing. In CIJ, pressurized flow undergoes Plateau-Rayleigh instability, breaking it into droplets [76]. Piezo crystals generate droplets through acoustic waves, and electrostatic or magnetic fields charge them. Charged plates deflect droplets as needed, with excess droplets recycled, as shown in figure 2(a). Although mature with advantages like high speed and nozzle clog resistance, it is limited to chargeable inks, and high speeds may compromise resolution.

Drop on demand (DOD) inkjet, in contrast to CIJ, releases ink only when it is required, eliminating the complex droplet charging, making it more economical. This allows for a smaller size of the droplet and a higher placement accuracy [80, 81]. It employs various pressure pulse generation methods, including thermal, piezoelectric, electrostatic, acoustic, electrohydrodynamic, and valve-based methods, as illustrated in figures 2(b)–(d), with thermal bubble and piezo crystal being the most common methods [82]. Thermal inkjet relies on rapid vaporization to generate an air bubble and eject droplets and has limitations with vaporizable inks and is prone to printhead degradation. Piezoelectric printheads use a vibrating piezo plate, offering better material compatibility and reliability. Valve-type printheads are another popular choice, which are versatile but may compromise resolution due to the pressurized release of fluid. In microfabrication of functional materials, piezoelectric DOD inkjet prevails, governed by voltage, pulse width, and nozzle vacuum. This section, therefore, focuses on the recent advancements in the fabrication of patterned microstructure arrays using DOD inkjet printing.

3.2. Droplet formation and impact

Realization of high-resolution features is only possible by controlling the droplet and how it impacts the substrate. Juxtaposed droplets tend to merge together if the impact velocity is higher and the splashing might also result in secondary droplets forming. While the fluid properties are crucial to this jetting, as shown in figure 2(e), it is also important to study droplet formation dynamics to ensure jetting stability and control the feature size. Typical droplet formation experiences several stages, focusing on the nozzle exit position and the leading droplet location. The ligament, the distance between the leading location and the nozzle before stream break-off, is a critical parameter. Efforts to study pinching behavior aim to eliminate tiny satellite droplets formed during tail breakup. As the satellite droplets are primarily formed by the tail breakup, they should merge with the primary droplet [83, 84]. External factors, like drag forces during high-speed printing, can lead to

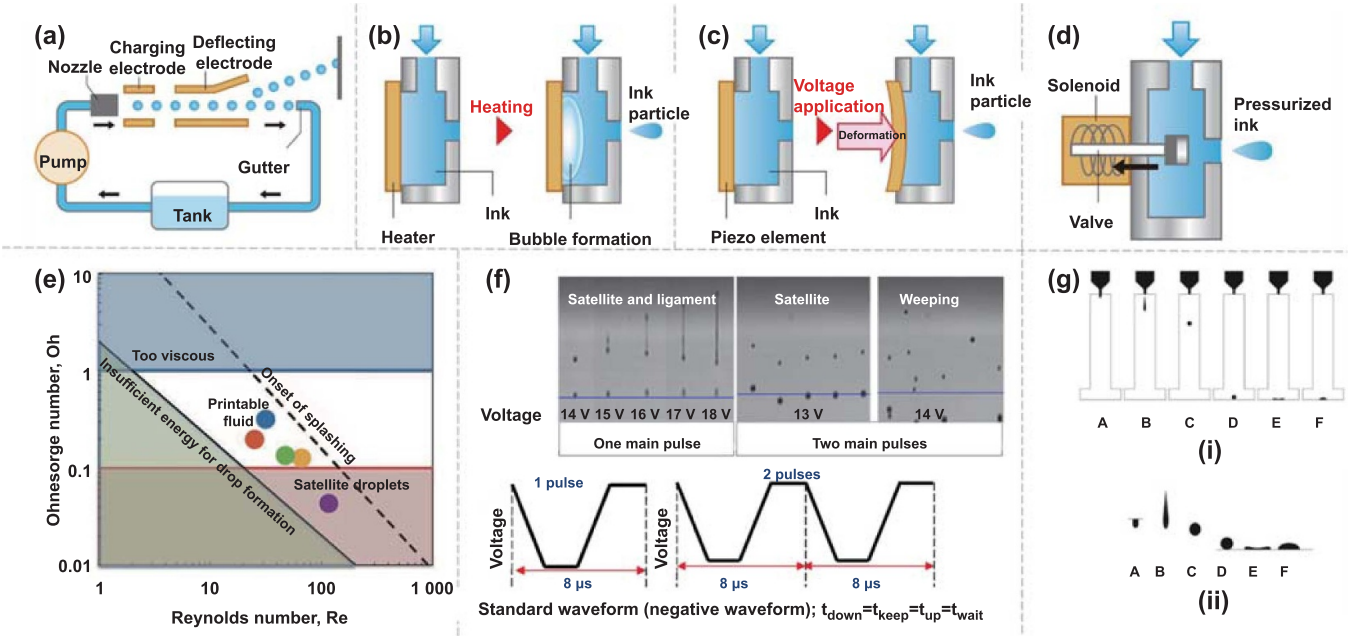

Figure 2. Types of inkjet technologies: (a) continuous inkjet; (b) thermal-based drop-on-demand inkjet; (c) piezo-based drop-on-demand inkjet; (d) valve type inkjet printing; (e) mutual dependence of Oh and Re for printability of fluids via inkjet. Reproduced from [77]. CC BY 3.0. (f) Droplet shape for inks using standard waveforms. Reproduced from [78]. CC BY 4.0, and (g) droplet movement (i) during inkjet printing when the droplet is ejected from the nozzle and settles on the substrate and the shape change at different stages, (ii) highlighted inkjet droplet phases at different stages. Reproduced from [79]. CC BY 4.0.

deviation and failure to recombine satellites with the primary droplet [85].

Active satellite elimination ways have also been long tested and developed, especially in piezo based printheads. Waveform design, which involves adjusting parameters like rise/fall voltage, rise/fall time, dwell time, and echo time, is widely used for achieving a certain jetting characteristic as shown in figure 2(f). A bipolar or unipolar signal is given as an input depending on the ink properties [86–90]. Experimental determination of optimal parameters is common, with rheology-dependent thresholds influencing droplet merging [91–94]. Bipolar waveforms are preferred for damping out vibrations, while unipolar waveforms offer stability with fewer satellites [95–99]. Waveforms are defined by the rise voltage, fall voltage, rise time, dwell time, fall time, and echo time, most of which are determined experimentally. A pressure control system adjusts backpressure for ideal meniscus for droplet formation [100]. Voltage effects on jetting behavior were studied by a lot of researchers, with material-specific voltage ranges [101–103]. The challenges at the nozzle tip due to the phase boundary are also contributors to partial clogging and non-ideal wetting affecting the jetting behavior [104].

An important aspect of inkjet printing is the way in which the adjacent droplets interact with the solid substrate and other droplets. Once the droplet is released from the nozzle, it strikes the substrate, and this impact on solid nonporous substrate causes various flow patterns depending on the properties of the ink and the substrate. Droplet impact and spreading depend on ink and substrate properties, jetting velocity, and droplet size, as shown in figure 2(g) [79]. Understanding the dynamic impact and equilibrium sessile drop state is essential for optimizing inkjet printing quality [105, 106]. The amount of spread is dependent on the surface energy of the substrate and was found to be dependent vastly on the Weber number [107–110].

3.3. *Material properties for stable jetting*

It is crucial to review the existing work studying the material properties of the inkjet materials as it plays a crucial role in determining the droplet resolution and consequently the resolution of the printed feature. Not all materials are suitable for ink jetting. Only the materials that have a certain viscosity and surface energy are printable. The material properties can be characterized by a set of dimensionless numbers like Reynolds, Weber, and Ohnesorge numbers (Re, We, Oh), and only materials within a certain range of these values are jettable, as shown in figure 2(e) [105, 111–114]. Achieving stable jetting often involves chemical modifications of inks. Adding solvents and surfactants is common for altering rheological properties without compromising functionality [115]. Inkjet printing of functional materials, often containing particulate matter, benefits from optimizing print resolution by controlling rheology and particle sizes. Nozzle clogging is addressed through impurity filtration and ink stabilization strategies [116]. Evaporating solvents, like ethanol, are popular for promoting jetting and higher resolution, but challenges like nozzle clogging may arise [117, 118]. Using solvent-specific dispersing agents is another approach used to ensure stable jetting and consistent droplets.

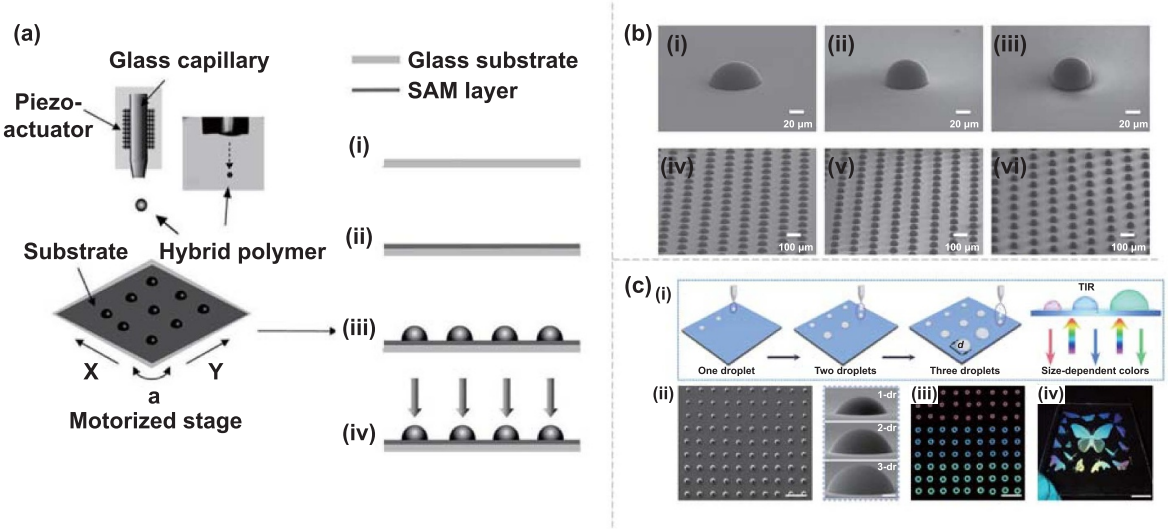

Figure 3. Different ways of fabricating microlenses. (a) Schematic of DOD inkjet printing used for microlens fabrication with the multi-step process (i) glass substrate, (ii) SAM layer, (iii) inkjet deposited microdomes, and (iv) UV curing for solidification. Reproduced with permission from [122]. Copyright 2011, Elsevier. (b) SEM images for a single droplet deposited on a CCVD-fluorosilane treated glass substrate with (i) 2, (ii) 4, and (iii) 8 flame passes and SEM image of an array of these microdomes printed using (iv) 2, (v) 4, and (vi) 8 flame passes. Reproduced with permission from [132]. Copyright 2020, Elsevier. (c) Facile color application of inkjet printed microlenses (i) schematic illustration of droplet-by-droplet printing with various microdome sizes realized by different number of droplets and the representation of size dependent TIR, (ii) SEM images of microdomes realized by changing the number of droplets, (iii) optical images of the realized structural color, and (iv) image printed with transparent ink using multi-drop approach with color realized due to the size-dependent TIR. Reproduced from [133]. CC BY 4.0.

3.4. Applications of DOD inkjet printing

Inkjet printing is at the forefront of micropatterning and has found applications in a variety of domains, including electronics, optics, filtration, water harvesting, cell scaffolds, and tissue fabrication, to name a few.

3.4.1. Microlens fabrication. Microlenses range from 5 μm to a few millimeters and find applications in a variety of applications like sensors, LEDs, communication systems, passive displays, etc. Surface finish and uniformity of individual microlenses play a crucial role in determining the functionality. While larger size of the microlenses is easier to fabricate with conventional processes, inkjet printing is more suited for smaller microlenses. As inkjet printing works by depositing tiny droplets of material, the dome shape can be naturally achieved by the virtue of the physical properties of the substrate and the interaction of the ink droplet with the landing surface. As the surface quality in this case is governed by the surface tension of the liquid, microlenses fabricated using inkjet printing have better surface finish. Furthermore, inkjet printing being more tunable, it is a suitable direct manufacturing method for fabricating microlenses with a high throughput at ambient conditions without the need for extensive postprocessing [119]. The use of UV curable resins for directly fabricating microlenses is an economical approach for large-area fabrication of microlens arrays (MLAs). MacFarlane's work on using molten polymers demonstrated feasible ways to fabricate convex microlenses using microdroplet jetting [120]. This work bolstered the use of inkjet printing in microlens fabrication and other opto-electronic applications. Ishii *et al* successfully established inkjet printing of UV-curable epoxy inks as an economical process for the fabrication of microlenses with diameters ranging from 20 μm to 140 μm [121]. When the liquid droplets are projected through the orifice, they strike the substrate and assume a partial hemispherical shape due to the surface tension, as shown in figure 3(a). UV irradiation solidifies these lenses. This method of fabricating MLAs has gained popularity as it requires no additional chemical treatments or processing. Microlenses obtained using this technique also exhibit superior surface finish [28, 122].

Tunability of the optical properties of microlenses has attractive applications in optical systems and other MEMS sensing devices. Different approaches to changing the NA of printed lenses were explored by many researchers. Changing the droplet size by manipulating the orifice and other jetting parameters was demonstrated in the late 90's to produce microlenses with different focal lengths [123]. While physical manipulation is easier to achieve, it is difficult to control the optical parameters in micro-steps. Thermal tunability of the printed lenses, as demonstrated by Parry *et al* showed feasible ways of changing the curvature and director profile of the lenses by manipulating the substrate. Their work also discusses thermal tuning of the optical properties of the lenses [124, 125]. Building on the concept of substrate modification for tunability, Kamal *et al* demonstrated the possibility of manipulating the optical properties of the microlenses by functionalizing the substrate to have electrical conductivity. The lenses showcased bifocal behavior when certain voltages were applied [126]. Material manipulation is another popular approach for achieving shape tunability in microlenses.

Hybrid materials with evaporating solvents have established themselves as powerful tools in the preparation of microstructured surfaces. Solvent evaporation leads to densification and results in changes in the final shape, focal length, and refractive index of the lens [127, 128]. Precise control of the solvent concentration allows for better control over the final shape. While the evaporating solvents are advantageous, the rapid evaporation leads to material pinning and the coffee ring effect [129]. This material pinning at the three-phase contact line creates micro craters, which although undesirable in most cases, can act as a guide for accurate droplet placement. Xia and Friend have used it to their advantage for producing patterned surfaces [130]. Despite the relative maturity, inkjet printed patterns can have inaccurate placements and relatively lower curvature profiles. Various multi-step strategies have been implemented to overcome the challenges with droplet placement. Droplet evaporation causes a ring-like structure to form, giving rise to microwells with elevated edges. This phenomenon is known as the coffee ring effect, which, although undesirable in most cases, has shown significant improvement in the placement accuracy and curvature control of the microlenses [131].

Inkjet-printed microlenses have been explored in various photonics applications. Single microlenses are deposited on optical fiber tips for coupling the light efficiently from diodes. They are also being used for collimating the light from lasers. Arrays of such microlenses arranged in specific configurations also allow for improved light gathering, making them promising candidates for optical I/O devices [29, 134]. Tien *et al* used inkjet to print MLAs with controllable fill factor on a light guide plate and achieved up to 82% light uniformity and 70% light efficiency [135]. Inspired by this work, researchers have used the approach to fabricate low-cost LCD backlights [29]. Zhang *et al* furthered this by providing ways to fabricate microlenses with high fill factor. In this study, MLAs were fabricated on an unstructured substrate with DOD technique using optimized UV inks on the top of self-assembled monolayers. These monolayers allowed the tunability of surface free energy, which helped with tuning the microlens' aspect ratio [32]. In a similar work, a team of Spanish engineers demonstrated the controllability of the microlens geometry by surface modification using chemical vapor deposition [132]. Microdome size and shape can be changed by changing the surface coating as shown in figure 3(c-ii). As their approach uses solvent-free ink, issues with the coffee ring effect can be eliminated. The approach is quite robust and can find immense applications in display technology and sensing. Utilizing hybrid polymers, Kim *et al* demonstrated the fabrication of MLAs with precise control over numerical aperture with applications in optical interconnects and pixelated image sensors [136].

As inkjet printing gives precise control over the dimensions of the jetted droplet MLAs with different defining characteristics can be printed in a single array. Exploiting this property, researchers created MLAs with tailored optical properties and multi-focal capabilities [137]. A similar approach was used to fabricate bio-inspired compound eyes with variable fields of view. This finds applications in medical imaging, large FOV optical components in astronomy, robotics, etc. Inkjet printing coupled with molding and air-assisted deformation was used to achieve the desired results [138]. Structural color generation has long been used by nature to generate colorful patterns by reflecting light at a particular angle. Microlenses can mimic the same effect by controlling the element size and the angle of incidence. While Goodling *et al* demonstrated the structural color using aligned polymeric microstructures, their fabrication method was complicated and lacked flexibility [139]. Li *et al* used inkjet printing to dispense microdroplets with varying sizes at predefined locations to generate photo-realistic images as shown in figure 3(c). Inkjet printing allowed for droplet placement flexibility and narrow droplet size distribution, ensuring color uniformity [140]. With their approach, they successfully demonstrated the tunability of different photographic aspects like gamut, saturation, and lightness just by the precise adjustment and placement of the microlenses with varying diameters. This approach has opened new avenues in imaging, biophotonics, and sensing.

3.4.2. Micropatterned structures for tissue engineering.

Micropatterns are characteristic of almost all the native tissues and organs. These functional micropatterns enhance mechanical properties as well as support other biological functions. Increasing interest in tissue engineering has forced researchers to look for scaffolds that can mimic these microstructures and allow precise cell placements for studying the interactions and tissue growth.

Piezoelectric DOD inkjet printing is widely used for biological applications due to its compatibility with a wide variety of biological materials [141]. Inkjet printing is being used for generating micropatterned structures as well as for depositing cell-laden materials on pre-patterned surfaces with high precision. Turcu *et al* used vinyl acetate and ethylene copolymer to create defined line micropatterns on gold, glass, silicon, and carbon substrates with 100 μm width. It was seen to direct the embryonic chicken neurons in the line orientation [142]. This method was further explored to produce collagen patterns. Roth *et al* printed dot, line, circle, and gradient micropatterns using a commercial bubble jet printer as a scaffold for cellular patterns using 350 μm protein patterns [143]. This approach was used to fabricate single-cell microarrays on hydrophobic substrates, which can be classified as living functional surfaces. Liberski *et al* used DOD inkjet to prepare sessile microdroplet arrays on oil-submerged surfaces, allowing for facile production of spatially addressable single-cell microarrays [144]. In a similar work conducted by Yusof *et al* they used DOD printing for printing single-cell arrays to be used as sensors for diagnostic and therapeutic applications [145]. Fujita *et al* used inkjet printing to produce a highly dense microarray of transfected cells for medical applications. They successfully produced 50 μm spots with 150 μm pitch that facilitated the screening and functional analysis of genes based on cell phenotype [146]. Cell culture environments like these are of increasing interest in bio-hybrid systems. Poly(L-lysine) was ejected using a single nozzle on a heated PMMA substrate to promote ink evaporation and

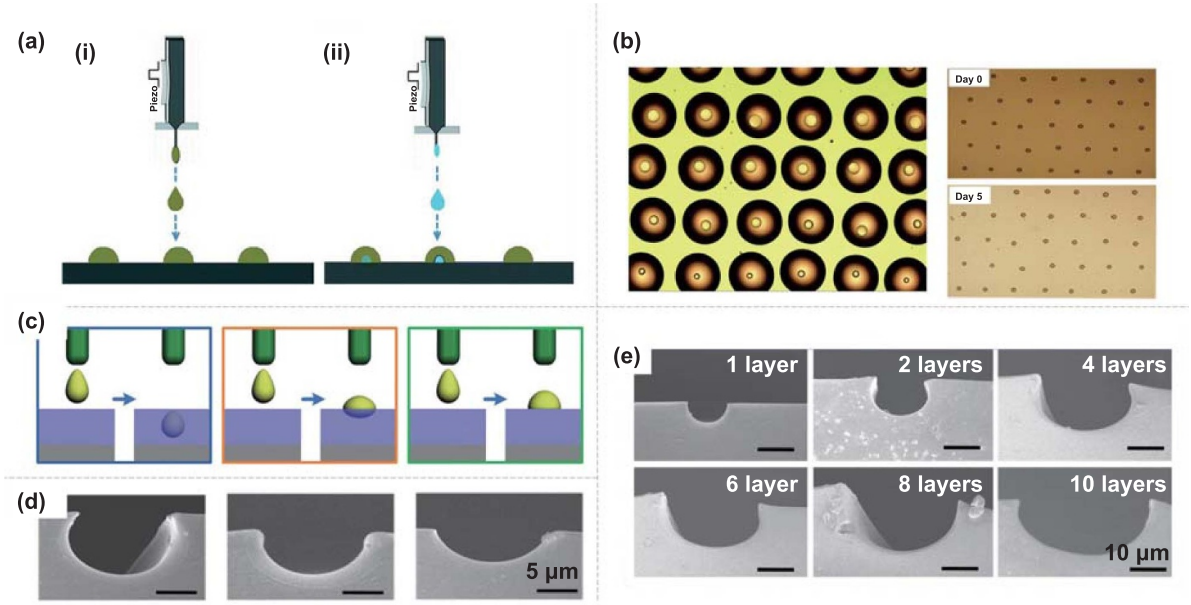

Figure 4. Micropatterning for tissue engineering. (a) Schematic of picolitre droplet-in-oil array fabrication by double-inkjet printing on a silicon dioxide solid support. (i) Oil droplet array formation. (ii) The PCR mixture is dispensed on the first oil microarray to produce the droplet-in-oil array. (b) Bright-field images (left) of multivolume droplet-in-oil array. From bottom to top, droplets were ejected at jet frequencies of 2 Hz, 4 Hz, 6 Hz, and 8 Hz. The final droplet volumes were 124 pL, 248 pL, 372 pL, and 496 pL, respectively. Bright-field images (right) of the droplet array sealed in the oil layer after standing at room temperature for 5 d showing no obvious changes in the droplet size as determined by the bright images. (a) and (b) Reproduced from [153] with permission from the Royal Society of Chemistry . (c) Schematic illustrations of three typical scenarios with printing inks onto viscous liquid surface, viscoelastic surface, and solid surface, respectively. (d) SEM images for microwells formed based on different levels of curing of the polymer substrate. (e) SEM sectional views of microgrooves fabricated with different printing layers. (c) and (d) [156]. John Wiley & Sons. © 2015 WILEY-VCH Verlag GmbH & Co. KGaA, Weinheim.

prevent blotting. Inkjet printing allowed the printing of parallel lines with widths ranging from 25 μm to 500 μm and concentric micro rings with increasing diameter. The flexibility provided by inkjet printing promoted production of freestanding protein arrays for applications in biosensing [147]. Inkjet printed scaffolds have shown promising results in guiding cell growth. A recent study by Sun *et al* used inkjet printing to produce micropatterns using I_3K nanofibers. Their results demonstrated that inkjet-printed peptide micro-patterns are effective in guiding cell alignment, showing great potential for nerve regeneration applications [148]. Similar work was previously presented by Gantumur *et al* where they developed a simple method using inkjet printing to create micropatterns on hydrogel substrates, making certain areas cell-adhesive and others non-cell-adhesive, resulting in aligned cell patterns. The system was capable of switching between different cell types as needed during cell growth [149].

Along with creating patterned surfaces, researchers have also successfully experimented with direct cell patterning on polymer substrates. Cell micropatterning essentially arranges cells with precision in 2D or 3D patterns to replicate complex tissue structures, enabling applications like drug screening and tissue engineering. These micropatterned cells are crucial for developing biomedical MEMS, organ-on-a-chip models, and personalized medicine point-of-care (PoC) devices [150]. This has been gaining popularity in the past two decades. Kim *et al* deposited sub-millimeter micropatterns using PLGA inks on a polystyrene substrate. The micropatterns were later loaded with stem cells for applications in developing customized functional tissues and other anatomically complex shapes [151]. Similar work was conducted by Matsusaki in which they successfully constructed HepG2 tissue microarrays using inkjet printing. They achieved spot sizes from 65 μm to about 2 mm by altering the number of droplets [152]. High-resolution protein patterns with diameters as small as 4 μm were achieved by using a superhydrophobic substrate. Using a 30 μm nozzle and evaporating additives, Sun *et al* fabricated patterned microchips for use as single-cell assays for real-time cellular apoptosis observations [153, 154]. Taking advantage of the high positional accuracy of inkjet printing, they employed a double jetting method. As shown in figure 4(a), mineral oil was jetted on an omniphobic substrate followed by the aqueous reagent. High droplet exit speed allowed the aqueous droplet to sink, and as seen in figure 4(b), the oil coating prevents the droplet evaporation, leading to a long-term stability of the cell culture. In a later study by Park *et al* a piezoelectric inkjet printer was used to pattern mammalian cells in a liquid-filled culture dish [155]. By optimizing printing parameters, they achieved a minimal positional error of $\pm$66 μm, making this technique valuable for cell patterning, sorting, and microarray fabrication. This innovative bioprinting approach not only combats rapid drying but also allows

for the creation of intricate cell patterns with gradients, mimicking natural tissues, thus finding significance in applications such as cell micropatterning and tissue engineering.

Researchers have printed negative features such as microgrooves and microwells for patterning cells and other functional materials. Using viscoelastic substrates that can deform in response to a particular ink, their morphology can be changed, making them suitable for fabricating concave microwells [157, 158]. The microwell sizes can be manipulated for forming single-cell arrays for cellular analysis. When the droplets impact the substrate, they cause indentation depending on the hardness of the substrate. Bao *et al* used viscoelastic substrates at different degrees of precuring to create controlled nanoindentation from the jetting droplets. Figure 4(c) shows that different indentation depths can be achieved corresponding to different viscosities of the dispensed inks. As depicted in figures 4(d) and (e), volatile material used for jetting multiple droplets evaporates, leaving behind different-sized microwells. These microwell arrays were used for patterning mammalian cells as the concave microwells have better wettability [156]. If the droplets are jetted close together, they merge to form continuous lines, which can be manipulated to form microgrooves. A cross-hatched microgroove pattern is important in microfluidic devices like microreactors [159]. Reactive solvents like toluene react with polycarbonate substrates to selectively etch the surface, forming concave cavities. By controlling the amount of this etchant, the size of the cavities can be tuned. Ban *et al* used this approach to fabricate arrays of hexagonal and circular microwells with 100 μm–170 μm diameters were fabricated. Surface treatments were used to induce wrinkles for enhanced cell adhesion [160]. Alongside the applications of micropatterned inkjet structures in cell and tissue research, it is also being widely used in pharmaceutical and drug delivery-related research. Scoutaris *et al* used inkjet technology to fabricate microdot arrays for providing controlled and predictable release of drug formulations. By dispensing sub 100 μm microdot arrays on hydrophobic substrates, a controlled drug dosage potential was demonstrated [161]. Inkjet is also used as a tool for coating the micropatterned structures at precise locations. Micropatterned structures were achieved using lithographic or other 3DP processes and were later coated selectively using DOD inkjet printing for applications in drug delivery and cell assays [161–165].

3.4.3. Hybrid printing techniques for functionalizing pre-patterned surfaces. Poor placement accuracy and droplet coalescence at high-density patterns inherent to inkjet printing can be addressed by providing a guide for the landing droplet. Using inkjet printing to precisely place droplets on prefabricated patterned substrates is a promising and widely used alternative for achieving the required feature density. Lithography is a popular choice for the initial patterning of the substrate. A pattern is first fabricated using lithographic processes and later used to guide the placement of the droplet as shown in figure 5(a). The surface energy of the jetted material restricts the droplet from falling off the pre-patterned micro platform [166]. A similar approach was later used to prepare a substrate for fabricating microlenses with tailored optical properties. The number of droplets that the micro platform can hold is determined by the surface energy. The number of droplets determines the curvature of the microlens, which in turn determines the optical characteristics [137]. As shown in figures 5(b)–(i), the number of droplets can vary the microlens structure, which in turn affects the focal length. Figure 5(c) shows the SEM image of the fabricated microlenses on lithographic patterns and the corresponding optical image with the bright spot at the focal point. Wang *et al* fabricated microlenses with controlled numerical aperture by following a similar two-step process. PDMS micro platforms were prepared by conventional photolithography. The material was jetted on each PDMS micro platform. The droplets were held together due to the surface energy, and with increasing droplet volume, the contact angle increases, causing change in the numerical aperture as seen in figure 5(d) [167]. A similar study was conducted to exploit the advantage of precise placement and solvent evaporation to produce lenses with high uniformity. Lithography was used to deposit a patterned hydrophobic layer of microwell array on a glass substrate, which was later filled with polyvinyl alcohol to produce microlenses with good focusing properties. The research presented a reliable approach to fabricating an array of convergent microlenses [168].

Inkjet printing's ability of precise droplet jetting finds applications in tissue engineering research. Micro cantilevers are fabricated using a lithography process and can be functionalized using various methods like spray-coating, pipetting, inkjet printing, and dimension-matched capillaries. Inkjet printing is advantageous for its spatial accuracy and high repeatability and allows area-wise functionalization of micropillar arrays [170]. Osteogenic markers were simulated on bioinert alumina micropillars by programmable loading of human stem cells using inkjet printing. The cellular response is determined by studying the amount of bending in the microcantilevers and micropillars. Precise placement with inkjet printing is being exploited in fabricating single-cell microarrays, multi-layer tissue chips, studying interfacial self-assembly in colloidal solutions, etc [144, 152, 169, 171]. As seen in figures 5(e) and (f), inkjet printing allows for a precise jetting of the cell cultures, allowing them to form desired tissue structures.

3.4.4. Micropatterned structures for controlled wettability. Inkjet technology, in combination with UV polymerizable resins, has been widely used for realizing some complex functional surfaces inspired from nature. Shark skin patterns have long been studied and used for achieving controlled hydrophobicity and self-cleansing properties. Wen *et al* used multi-jet inkjet, multi-material inkjet printers to fabricate flexible surfaces with rigid denticle patterns mimicking shark skin structures as shown in figure 6(a) [172]. Use of inkjet printing allows for the material flexibility. The shark skin patterns as observed in nature are complicated to replicate as it is even using AM technologies. These patterns are therefore studied and their crucial features contributing to the desired properties

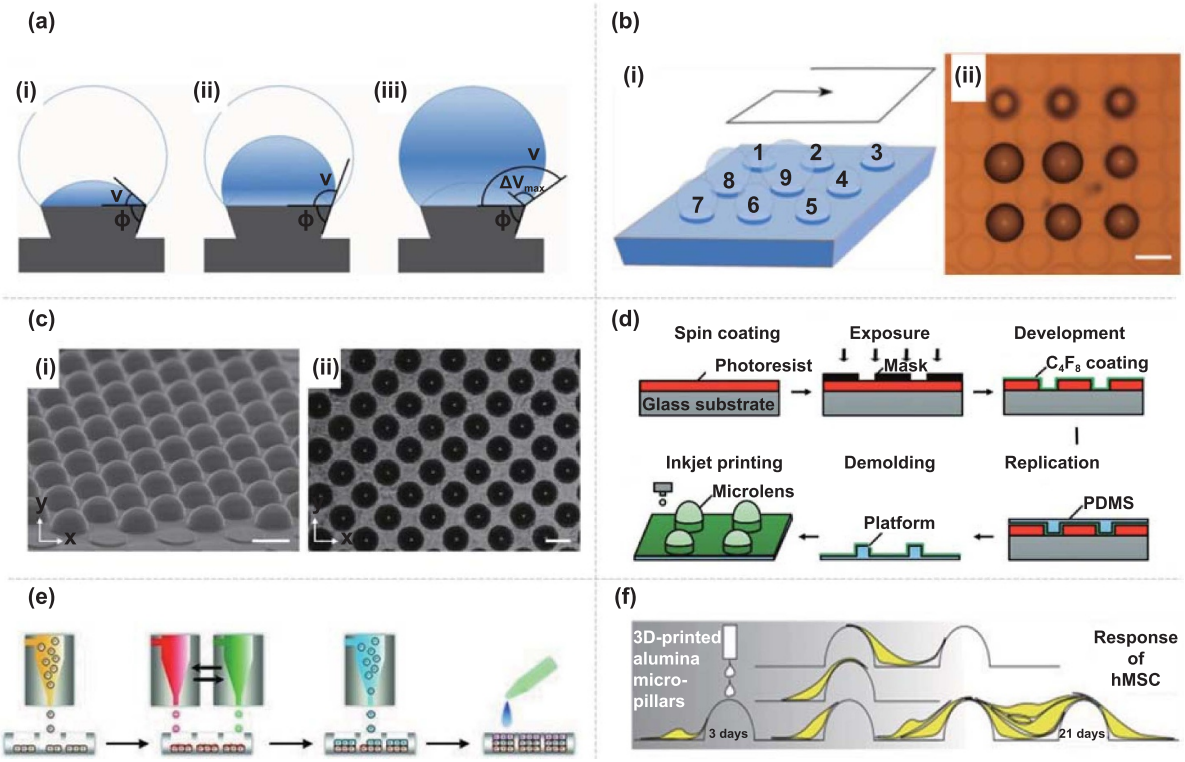

Figure 5. Hybrid printing techniques for realizing functional surfaces. (a) Scheme of a drop confined on a platform with a lateral dimension smaller than the capillary length. (i) The minimum value of the edge angle ν is equal to the contact angle θ; (ii) increasing the drop volume, the edge angle minimum value increases; (iii) the maximum value of the edge angle depends on the contact angle and the angle of the platform rim, ϕ. Reproduced from [166]. © IOP Publishing Ltd All rights reserved. (b) MLA with 9 different microlens specifications: (i) schematic of the array, (ii) optical top view showing the microlens height varying with the volume increase from platform to platform. (c) Microlens arrays (i) SEM image of a part of the cross-linked MLA. (ii) Optical image of the focal plane showing the individual microlens focal points. (b), (c) Reprinted from [137], © 2018 Elsevier B.V. All rights reserved. (d) Illustrative steps of the micro platforms fabrication process. Reproduced from [167]. CC BY 4.0. (e) Schematic illustration of the development of 3D micro-tissue arrays by the layer-by-layer printing of single cells and proteins [152]. John Wiley & Sons. Copyright © 2013 WILEY-VCH Verlag GmbH & Co. KGaA, Weinheim. (f) Response of hMSC on 3D printed alumina micro-pillars. Reprinted from [169], © 2016 Acta Materialia Inc. Published by Elsevier Ltd All rights reserved.

are incorporated into designs that comply with the design for manufacturability principles. Their later study also studied the relation between the spacing between the individual shark skin features and their influence on the hydrodynamic properties of the patterned surface. The realization of these surfaces with controlled spacing between the individual microstructures was possible only due to the advancements in multi-material DOD printing [173].

The principles of selective hydrophobicity were also used by many researchers for fog harvesting applications. Nishimoto's approach utilized inkjet printing to create superhydrophobic patterns on a superhydrophilic substrate. Their approach dip-coated titania anatase to create the substrate, followed by surface modification with self-assembled monolayers and ink jetting to create patterns using aqueous UV-resistant inks. Upon exposing the surface to UV light, the self-assembled monolayers underwent photocatalytic decomposition, resulting in the desired pattern that was obtained after the water-washing step [176]. The patterns on the back of the Namib beetle were replicated on a large scale using a direct single-step mask-free approach. Zhang *et al* prepared a superhydrophobic substrate and later patterned dopamine solution using DOD inkjet technique [174]. These surfaces with a pattern size of 500 μm and a separation of 1000 μm have shown a high amount of water retention capacity as shown in figure 6(b), providing viable solutions for fog harvesting in the thermal desalination process. Moreover, Song's research group used inkjet printing to produce a myriad of superhydrophilic–superhydrophobic patterned surfaces, offering potential applications in water-harvesting [177, 178]. It was also explored for printing Ag nanoparticles to produce high-resolution conductive patterns, micro-colloidal crystals, and photonic crystal patterns consisting of dot and line patterns [175, 179, 180]. Inkjet printing is advantageous in precise patterning of hydrophobic crystals, as shown in figure 6(c), which aid with self-assembly.

4. Light-based techniques for surface micro-texturing

Despite the numerous advantages that inkjet printing offers, it still has a fair number of challenges when it comes to printing micropatterned functional surfaces. As this process

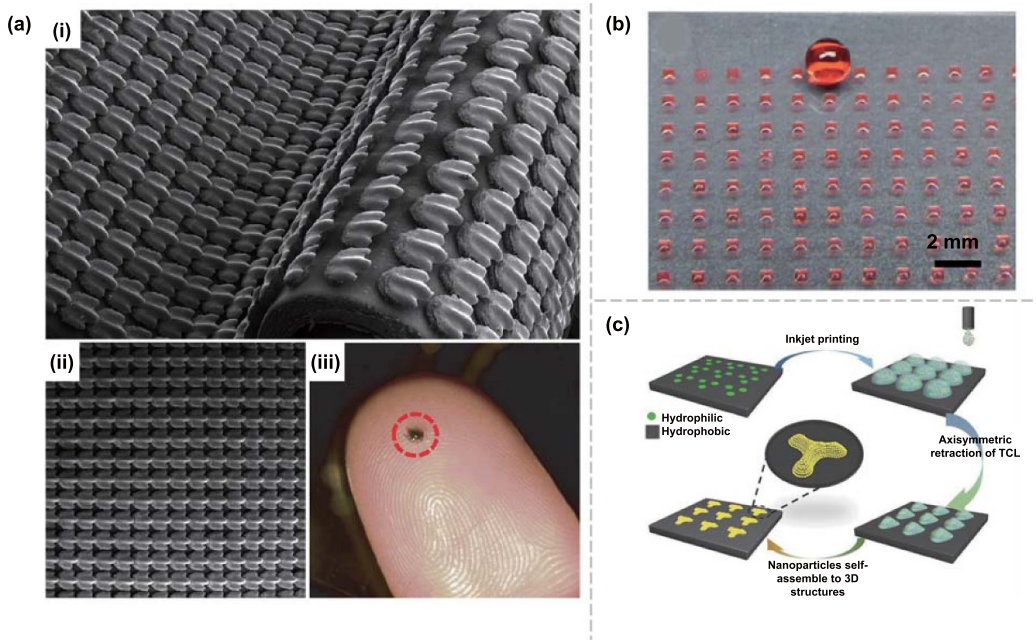

Figure 6. Micropatterned surfaces for controlled wettability. (a) Printed shark skin pattern. (i) SEM image of the synthetic shark skin membrane printed using multi-jet printer, (ii) patterned placement of the denticle pattern, and (iii) individual shark skin denticle. Reproduced with permission from [172]. © 2014. Published by The Company of Biologists Ltd. (b) Image showing water droplet accumulated on inkjet printed hydrophilic polydopamine patterns (500 μm squares) on a hydrophobic substrate. Reproduced from [174] with permission from the Royal Society of Chemistry, and (c) printing of patterned photonic crystals on a hydrophobic silicon wafer with hydrophilic micropatterns realized using DOD inkjet printing [175]. John Wiley & Sons. © 2015 WILEY-VCH Verlag GmbH & Co. KGaA, Weinheim.

relies on droplet ejection, factors like ambient temperature, air flow, etc., make it difficult to control the consistency of the deposited droplets. Most inks use solvents that promote jettability and evaporate once the droplet leaves the nozzle. The uneven evaporation and the inter-phase boundary conditions can cause inconsistency in the printed patterns. The limited availability of materials poses another challenge. Many of the functional surfaces found in nature have microstructures that have complex 3D geometries such as overhangs, loops, curvatures, etc. Inkjet printing is more efficient when printing concave or convex structures like microwells or micro domes. In order to unleash the complete potential of these biomimetic designs, it is necessary to replicate each individual element with precision rather than just replicating the pattern placement. Light-based systems are capable of fabricating complex 3D microstructures, which can mimic nature and fabricate a wide array of possible geometries. Amongst the light-based techniques, two-photon polymerization (2PP) and stereolithography (SLA) are the most popular approaches. While 2PP offers extremely high resolution, it is limited by the size and speed of fabrication. Micro SLA printing can address most of these challenges and is thus becoming increasingly popular in the microfabrication community.

4.1. Fundamentals of MicroSLA printing

High-resolution 3D printing is realized by localized photopolymerization of liquid resin that solidifies the resin in response to UV light. This can be achieved using two-photon polymerization (TPP), SLA, and DLP techniques [6, 50, 181–184]. TPP uses ultrafast high-energy pulsating lasers with longer wavelengths to provide a high flux of photons at localized regions, which solidifies the resin. As solidification can only occur when two photons are absorbed at the same time, TPP has a very high resolution. SLA is also a laser-based process that uses a rastering UV laser to selectively polymerize the resin. As both these techniques use scanning lasers that induce local photopolymerization at the point of illumination, they are relatively slow. On the other hand, DLP-based 3D printing performs local photopolymerization by projecting 2D UV patterns on the resin surface, the schematic of which is shown in figures 7(a)–(c). As this technique offers high resolution at elevated speeds, it has become a popular choice amongst researchers for microfabrication [183, 184]. Compared to other light-based AM technologies, DLP covers a broader range of resolutions and can print over a relatively wider area by adjusting the magnification of the projection lenses [185, 186]. This makes it a popular choice for the fabrication of micropatterned functional surfaces.

Sun *et al* developed the very early versions of projection-based microSLA setup using a digital micromirror device (DMD) to generate digital masks [183]. The process fabricates complex 3D structures in a layer-by-layer fashion. This is advantageous over inkjet printing as it has the ability to fabricate complex, overhanging, and morphologically diverse structures with relative ease. A 3D CAD model is first sliced in a sequence of 2D images that are later transferred to the DMD chip. UV light illuminated on the DMD is modulated by the input signal, and the corresponding 2D patterns are projected on the vat containing resin. Each individual micromirror

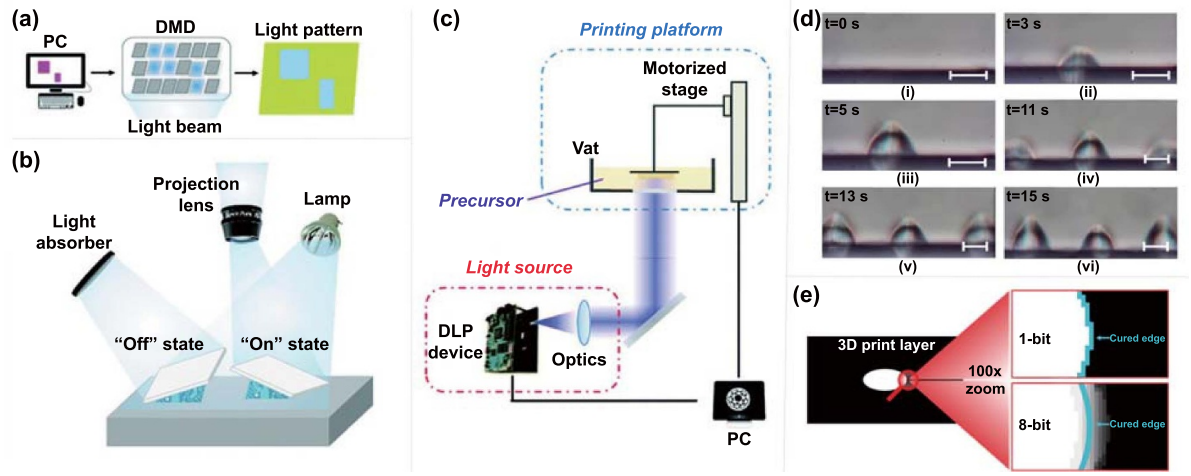

Figure 7. Scheme of DLP-based 3D printers. (a) A typical process to generate patterned light fields using DMD, (b) the working mechanism of individual elements on a DMD chip, (c) a representative setup of DLP-based printers. Reproduced from [187] with permission from the Royal Society of Chemistry, (d) 3D voxel growth observations in DLP 3D printing. Reproduced from [188]. © Laboratory for Freeform Fabrication and University of Texas at Austi, and (e) schematic showing the effect of grayscaling on spatial resolution in DLP printing.

switches between on and off state at a high frequency to reflect light in response to the desired pattern. The patterned UV light initiates local photopolymerization on the surface of the resin, which solidifies the resin. The translational stage moves the platform, introducing fresh resin, and the process repeats until the entire structure is fabricated.

4.2. Theoretical foundations for photopolymerization kinetics

Photopolymerization, a form of free radical polymerization initiated by light, is widely used in applications like surface coatings, biomedical, and AM. This process boasts advantages such as faster polymerization rates, lower energy consumption, and sustainability. Photoinitiators in the resin mixture decompose upon irradiation, activating polymerization [189]. The depth of polymerization is limited by light penetration, inversely proportional to photoinitiator concentration. The cure depth is always less than the penetration depth, following Beer-Lambert's equation [190–192]. This technique is suitable for thin film applications and layer-by-layer solidification processes, making it ideal for 3D printing.

First documented in 1845, photopolymerization has evolved, with Chuck Hull introducing the SLA process in 1986 [193, 194]. Objects with resolutions as low as 10 μm can be printed, finding applications in various fields [6, 195]. The DLP method, based on the same principle, uses a light source to illuminate entire layers simultaneously, reducing build time. DLP technology, relying on a DMD chip, allows tuning of feature size through optics manipulation. Parameters like light intensity, wavelength, exposure, and light-material interactions influence the process [196–198]. Zhou *et al* found that lateral resolution is governed by input irradiance, with light bleeding into neighboring pixels due to diffraction inefficiency and dark-field diffusions, particularly at higher resolutions [199–202]. The photopolymerization kinetics works significantly differently at different scales. The current work by Chivate *et al* on developing an observation-based empirical relation between light intensity and spatial spreading has significantly improved the understanding of photochemical kinetics at the micron scale. The schlieren-based observation of voxel growth as seen in figure 7(d) has led to the development of more robust photopolymerization models that have alleviated our understanding of light spreading at a tiny scale [203, 204].

4.3. Voxel growth and grayscaling strategies

Detailed investigation of the voxel growth dynamics is necessary, especially at micron scale as it is a determining factor in the resolution of the printed feature. Based on the application and the shape of the desired microstructure, the part can be fabricated either with a layer-by-layer approach or by monolayer photopolymerization. Both of these methods have their own merits. Monolayer photopolymerization is a popular choice for fabricating parts with a freeform surface using a single exposure shot. Microlenses and microneedles are commonly fabricated using this technique [205, 206]. The part is grown by controlling the exposure and energy distribution. The cured profile of the resin follows the light energy distribution. As the light reflecting from a single micromirror is Gaussian, the cured profile for a single pixel is also Gaussian, and multiple pixels follow a flat top Gaussian profile [46, 48, 201]. Minor deviation from the ideal Gaussian profile is attributed to the complex light-matter interactions. The spatial resolution is governed by the spreading of light. Light spreads into neighboring pixels due to diffraction inefficiency and dark-field diffusions [200]. For a larger number of pixels, the cured profile matches the projected image quite well in the lateral direction, but for a smaller number of pixels, the cross-talking is significant, causing shape distortions. Binary images modulate the micromirrors in only two states: 100% on and 100% off, which result in the cured profile mirroring the light intensity profile in the lateral direction. As the DLP contains a finite number of pixels, the projected mask approximates the desired

shape with a resolution defined by the individual micromirror size. This approximation can alter the desired shape, especially at the micro-scale. Further imperfections are introduced due to focusing and diffraction [183]. The light from an individual micromirror typically spreads into neighboring pixels. Therefore, the effective light exposure per unit area is greater for larger projections. Light spreading for smaller features results in lower net exposure, causing the smaller features to fail [207]. This is desired in all applications, especially when the cured profile is significantly different from the projected image and the corresponding light intensity curve. Effect of light spreading and feature proximity on the resolution was quantified by Chivate *et al* The voxel-voxel interactions as a result of the proximity were observed in-situ for the first time as seen in figure 7(d). Their work presents a novel strategy to overcome the negative effects of light spreading and introduces a multi-mask strategy for printing high-resolution features [208].

Grayscaling is a crucial factor in layer-by-layer fabrication as well as achieving good spatial resolution [209, 210]. The profile can be controlled by adjusting the light exposure, which is possible by projecting grayscale images as shown in figure 7(e). The percentage of time spent in each state determines the grayscale level [211]. Monolayer photopolymerization is widely used for fabricating MLAs, where it is critical to control the shape of the cured profile. Grayscaling is helpful for improving the projection and more accurately producing a feature without having the need to increase the resolution of the DMD [209]. However, accurately obtaining the cure profile with grayscale alone is challenging. A thorough understanding of oxygen inhibition, thermal shrinkage, self-focusing, and photo-bleaching can potentially aid in predicting the shape and dimensions of the final profile. Mathematical and empirical models that can predict the shape of the cured profile for a single exposure photocuring based on the input parameters like exposure, wavelength, and photochemical reactions have been developed [46–48, 204, 212–214]. These models are helpful in fabricating microlenses and microneedles with relatively high aspect ratios. Despite the numerous advantages of monolayer fabrication, it can only be used to fabricate parts that have lateral dimensions within the curing depth. It is not the best approach for fabricating high aspect ratio structures and complex 3D microstructures. Layer-by-layer approach is widely used for fabricating microneedles, biomimetic structures, micro springs, and other micro devices [183, 184, 215, 216]. It is advantageous as it can overcome the cure-depth limitations by slicing multiple thin layers and moving the build plate step-by-step until the desired structure is realized. Despite these advantages, the layer-by-layer approach causes staircase effect inducing surface roughness which might not be desirable [217]. Efforts have been made to eliminate this effect by changing the photopolymer formulations, using defocused image patterns, and inducing external oscillations [206, 218–220]. Thinner layers have been used for mitigating the staircase defect and to achieve smoother surfaces, but these methods tend to be slower [221, 222]. Carbon Inc. introduced a smarter continuous liquid interface (CLIP) 3D printing which uses multiple images as a video projection while the stage moves continuously. This has helped achieve faster speeds, higher resolution, and smoother surface finish [222]. Micro-CLIP is now being used for fabricating microstructure arrays with desired surface finish [223].

4.4. Applications

Micropatterned surfaces have been used for a wide variety of applications owing to their exceptional attributes. These finely crafted surfaces are capable of achieving a wide variety of functionalities like chemical separation, antibacterial properties, optical enhancements, and targeted drug delivery. Traditional methods often encounter challenges while crafting these intricate surfaces. The intricacies of micropatterning require high precision and details, which is often inefficient, time-consuming, and uneconomical when using conventional processes. DLP printing has transformed functional surface manufacturing with applications in healthcare, optoelectronics, and biomedical fields. By harnessing the power of light, it offers a novel and highly efficient approach to microfabrication.

4.4.1. Fabrication of MNA. Microneedles are devices designed for the purpose of epidermal and intradermal delivery of vaccines and biomolecules, and also for sensing applications. Microneedles can be broadly classified into hollow, coated, porous, soft, solid, and dissolvable formats featuring complex shapes like conical, arrowhead, etc [224]. Although conical geometries of microneedles are widely used, researchers have shown the benefits of using tapering tips, pyramidal, and rectangular shapes as well. Bio-inspired geometries are becoming increasingly popular due to the improvements in materials and fabrication processes, especially DLP printing, which is making the realization of high-resolution complex biomimetic geometries possible. Although TPP provides higher resolution, DLP printing is widely preferred for its high throughput, lesser susceptibility to oxygen, and lower cost [225]. DLP technology has long been employed for the indirect fabrication of MNA, wherein it is a part of micromold fabrication. DLP printing is used to fabricate microneedle masters, which can later be imprinted onto PDMS substrates to produce micromolds. Johnson and Procopio used this strategy to fabricate microneedle masters [226]. These micromolds are later used for fabricating MNA using bio-compatible materials. As the microneedles were fabricated layer-by-layer, staircase finish was observed irrespective of the layer thickness, with the tip radius larger than designed geometry. Microneedle truncation was observed, with actual sizes being 30% less. The CLIP-based system provided smoother surfaces but did not eliminate truncation effects [227]. Gradient-based grayscaling was utilized to overcome these challenges. Commercial DLP printers can adjust the grayscale automatically to accommodate the truncation error. The fabricated MNA was used for templating onto silicone, which was later baked to prepare a mold. Micromolds have been used as a template for fabricating dissolvable MNAs with nanoparticle loading. This templating capability allows for the use of biocompatible materials that may not be easy to photopolymerize [228–230].

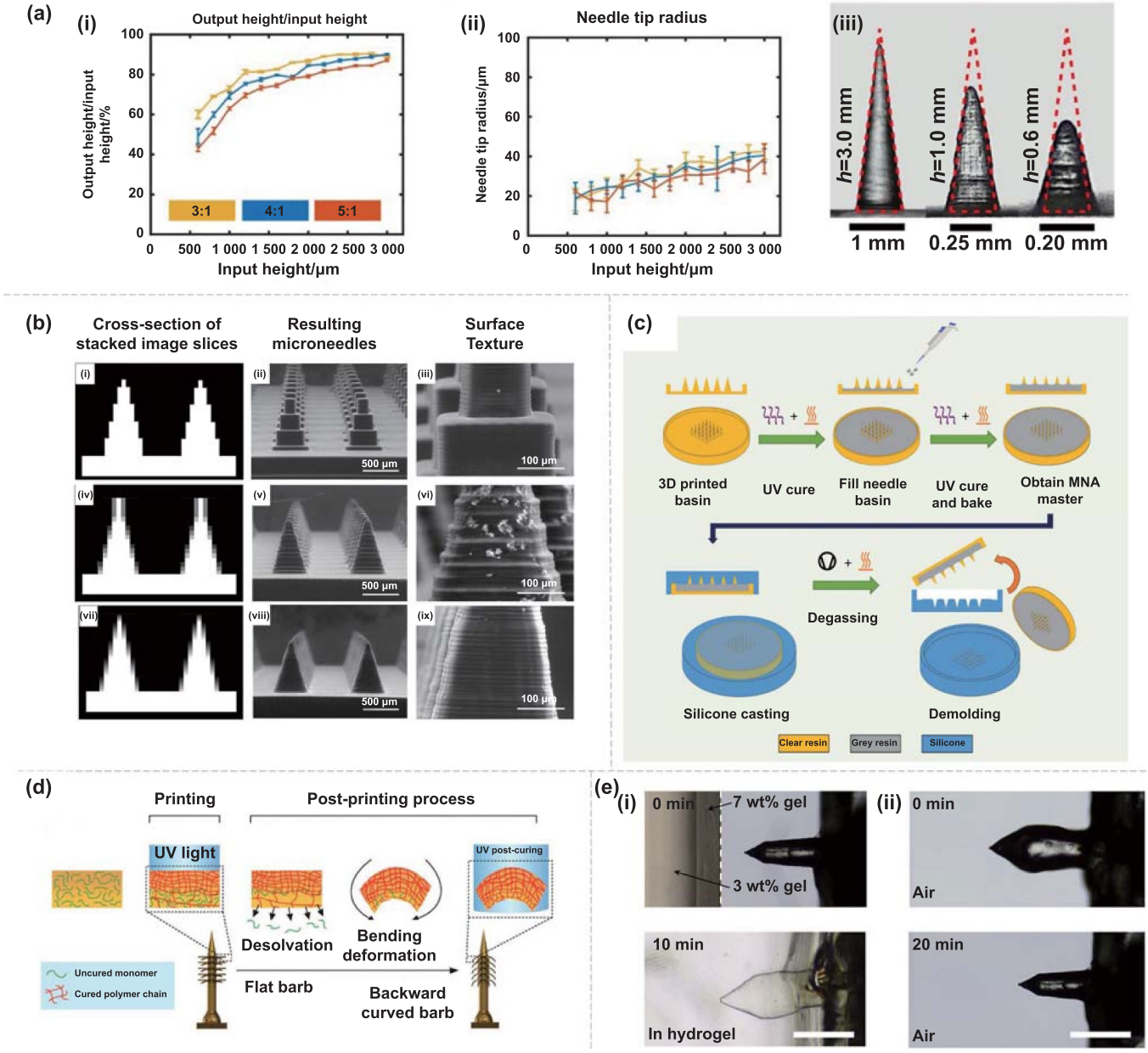

Figure 8. Microneedle array fabrication. (a) Comparison between different microneedles. (i) Output-to-input height ratio; (ii) needle tip radius with changing input needle height, (iii) Needles with an aspect ratio of 4:1 with input height 3 mm, 1 mm, and 0.6 mm with the theoretical dimensional of the needle outlined in red. Reproduced from [230]. CC BY 4.0. (b) Stacked-images cross-section, SEM images at low and high magnification for (i)–(iii) microneedles fabricated with binary images, (iv)–(vi) printed with printer's default grayscaling algorithm, and (vii)–(ix) printed with optimized grayscaling algorithm. Reproduced from [226]. CC BY 4.0. (c) Fabrication process for microneedles with stereolithography 3D printing and replica molding method. Reproduced from [230]. CC BY 4.0. (d) Schematic illustration of 4D printing approach to program deformation of horizontally printed barbs into a backward-facing shape. Reproduced with permission from [237]. CC BY-NC 4.0. (e) Swelling/deswelling behavior of the swellable MN with 60% swellable tip height. Time-lapse optical images for (i) swelling of the MN following insertion into the multi-layered hydrogel prepared using different agarose concentrations (0 and 10 min) and (ii) deswelling in the air after removal from the hydrogel (0 and 20 min). Scale bar represents 500 μm. Reprinted from [236], © 2017 Elsevier B.V. All rights reserved.

Despite the grayscaling, it was observed that with increasing input height, the produced feature was closer to the actual height and the tip size was larger as seen in figures 8(a) and (c). This can be attributed to the fact that needles with more height have a relatively higher total energy exposure, allowing a greater amount of photopolymerization to take place. By utilizing appropriate materials for creating the molds, the size of the replicated microneedles can be altered. Hydrogels exhibit isotropic shrinkage upon evaporation. Negative micro molds prepared by templating the 3D printed MNAs onto hydrogel can later be miniaturized, casted and a new master can be prepared. This allows for finer features with precise control over the microneedle size, and Ochoa *et al* could achieve microneedles with tip sizes less than 10 μm

[231, 232]. With advancements in the materials and DLP process, direct fabrication of microneedles has also been proposed. Yao *et al* demonstrated the use of customizable resins with high functional material loading for direct fabrication of MNAs. They fabricated microneedles with microporous hydrogels that were soaked in the drug solutions [233]. Utilizing reverse approach, the potency of the method for drug detection was successfully studied. This approach has also been used for fabricating personalized microneedle patches with customizable drug loading and is increasingly being used in PoC medical services [234]. Although the mechanical strength of the direct fabricated MNAs is debated, various post-curing techniques have been evolved to enhance the mechanical strength. Uddin *et al* fabricated microneedles with cross-shaped cross-sections and post-cured under UV radiation to enhance mechanical strength. These have been used as drug carriers for oncological purposes. The cross-shaped design allowed to increase the drug loading [164]. Following the same fabrication regime, similar studies with different needle geometries have been conducted. Direct fabrication has the potential to fabricate programmable microneedles possible with AM and has demonstrated increased drug loading and tissue adhesion. 3D printing with programmed shape deformations is known as 4D printing and is a popular approach for producing bioinspired microneedles.

Khan *et al* demonstrated a smart way of fabricating 4D printed microneedles with barbs that curve in response to curing. This backward bending of the barbed structure as shown in figure 8(d) allows for better drug delivery [237]. Similarly, Han *et al* printed microneedles with reversed barb structures that demonstrated 18 fold increase in the adhesion of microneedles [235]. They exploited the cross-linking density gradient in photocurable polymers and controlled the material parameters to induce exposure-controlled bending. Seong *et al* demonstrated bullet-shaped microneedles with swellable geometry. Shape change was introduced by swelling of the prepared multilayered hydrogel matrix. The prepared microneedles swell and de-swell in response to a water-rich environment, which is helpful for drug loading. Swollen microneedles can be freeze-dried to create structures with internal pores as evident from figure 8(e) [236]. Limpet tooth-inspired MNAs were demonstrated by Chen's group, where they used iron oxide reinforced resin to enhance the compressive strength. Magnetic field-assisted alignment was used to achieve anisotropic properties and tunability of mechanical properties [238]. The ability of CLIP-based methods to rapidly and directly fabricate MNAs of different shapes, sizes, aspect ratios, and compositions was demonstrated by Johnson *et al.* This method could successfully fabricate multi-material microneedles by switching the resin vat mid-printing. This work demonstrated a more versatile and fast fabrication technique for MNAs [227]. Lee *et al* demonstrated 30 μm micro-CLIP printing by optimizing the projection parameters and using a 30 μm resolution printer. The researchers used iterative methods to extract printing parameters for each layer and optimized them dynamically to achieve desired lateral and vertical resolution with high repeatability [223].

4.4.2. Microlens fabrication. Conventional methods for microlens fabrication are time-consuming, and inkjet printing has its own limitations. Micro DLP printing presents a cost-effective, facile, and fast fabrication technique. Contrary to MNA fabrication, the use of DLP printing for fabricating negative molds for producing MLAs is not very popular. The layer-by-layer approach introduces a staircase finish on the microlens surface, which affects the optical properties. Although grayscaling can eliminate this effect to a certain extent, optical smoothness is desired to achieve high optical properties. Chen *et al* proposed a grayscale photopolymerization technique coordinated with meniscus equilibrium post-curing. Sub-voxel resolution with a significant reduction of the staircase finish was observed with surface roughness as low as 7 nm without slowing down the process [239]. Alternatives to layer-by-layer fabrication can provide better control over the cured profile. Shao *et al* used a customized micro-CLIP system with grayscale masks to produce up to millimeter-scaled microlenses with high surface smoothness while eliminating the recoating/meniscus equilibrium stages [240]. Using grayscale photopolymerization, production of microlenses with single-exposure UV curing was demonstrated by Emami *et al* [48]. They proposed a process planning framework based on Jacob's curing curve and other light resin interactions to generate grayscale patterns. Freeform voxel was cured by illuminating the generated grayscale pattern through a transparent substrate and was later cleaned gently, followed by UV post-cure to retain the profile as shown in figure 9(a) and as discussed in their previous works. Kotz *et al* used a similar principle of grayscale single-exposure lithography to fabricate fused silica glass microlenses, which were later heat-treated to form an array of glass microlenses. AM compatible process with high fidelity fused silica glass manufacturing was demonstrated that has found application in fabricating MLAs and other patterned structures [241]. Many applications demand optically smooth surfaces, which are not always possible even with single-shot exposure AM. Yuan *et al* proposed oscillation-assisted techniques to fabricate high-fidelity, optically smooth microlenses with surface roughness close to a single nanometer. Computationally generated grayscale and high-frequency vibrations induced by the projecting lens were used to fabricate convex as well as concave microlenses with desired focal lengths [206] as shown in figures 9(b) and (c). Grayscale alone might not be sufficient to achieve high surface finish microlenses. In addition to the grayscaling, scientists have implemented post-treatment approaches like meniscus equilibrium post-curing, where they combine SLA printing with meniscus coating to cover the layers to achieve a smooth surface as shown in figure 9(d).

4.4.3. 2.5D micro-structure array fabrication. Structures that can be designed by extruding a 2D image without any further modifications to the geometry are classified as 2.5D structures and find applications in cellular and drug response research. Although conventional lithography is a common fabrication practice, the limitations on the aspect ratio make it challenging

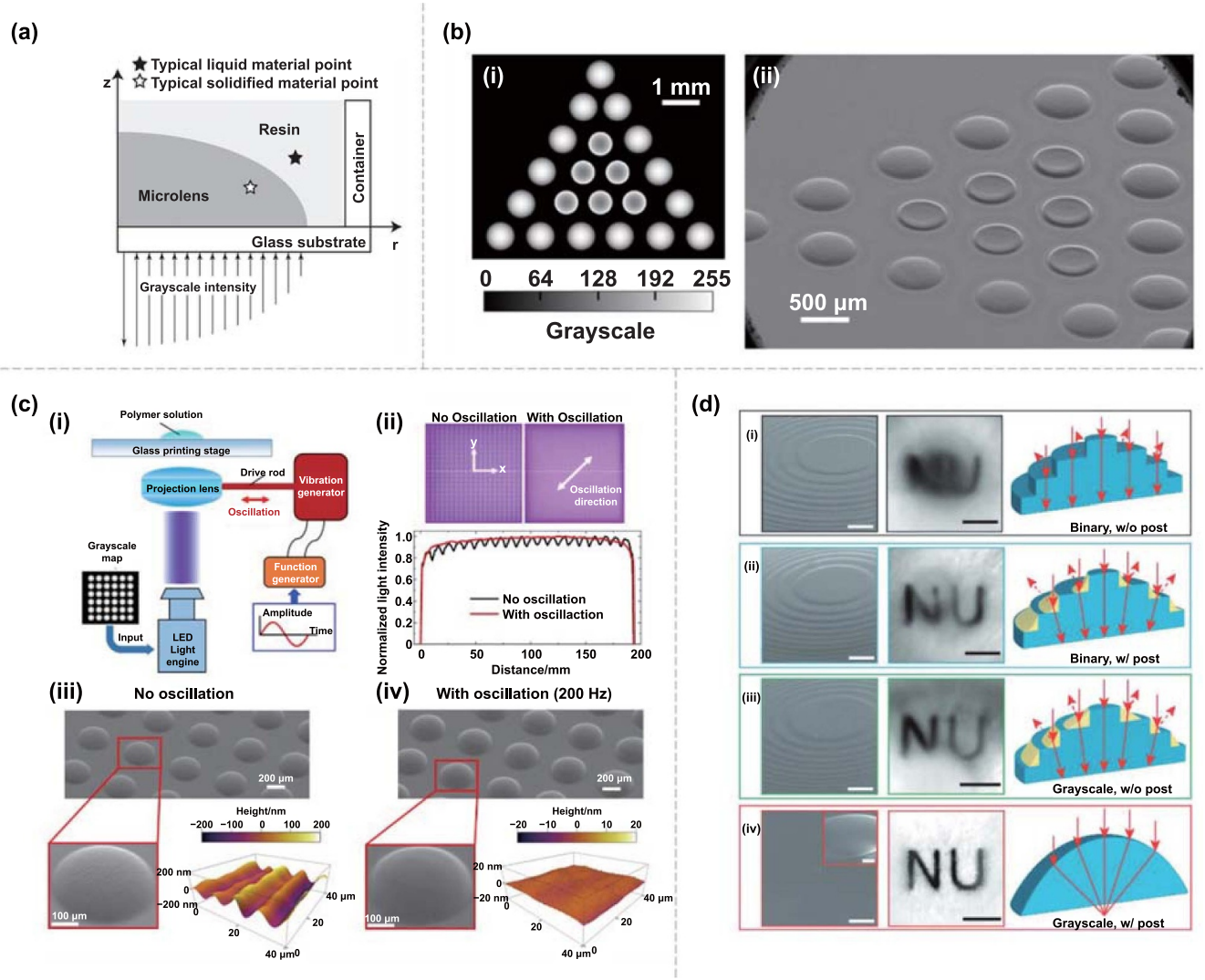

Figure 9. Microlens fabrication using DLP based printing. (a) Schematic of an axisymmetric cross-section view of grayscale light intensity and corresponding cured profile. Reproduced from [46]. © Laboratory for Freeform Fabrication and University of Texas at Austi. (b) Effect of grayscaling on printed pattern (i) Grayscale map with the hybrid grayscale design. (ii) SEM image of the hybrid microlens array. (c) Fabrication of microlens array by an oscillation-assisted DLP-based printing system. (i) Schematic of the oscillation-assisted DLP-based printing system. (ii) Comparison of the projection pattern (200 μm $\times$ 200 μm) and normalized light intensity distribution between non-oscillated and oscillated projection, (iii) and (iv) SEM and AFM characterizations of the microlens arrays fabricated under non-oscillated and oscillated projection. Reprinted with permission from [206]. Copyright 2019, American Chemical Society. (d) Effect of different post-curing processes (i) Lens printed by binary patterns without post-curing process, (ii) lens printed by binary patterns and the following meniscus equilibrium post-curing process. The polymerized meniscus structures are illustrated in yellow, (iii) lens printed by grayscale photopolymerization without the meniscus equilibrium post-curing process. As illustrated in yellow, the grayscale polymerization provides a smooth transition from the pixelated roughness, and (iv) lens printed by grayscale photopolymerization and the following meniscus equilibrium post-curing process. The first column in panels (i)–(iv) shows SEM images of the surface of the printed lenses. Scale bars: 200 μm for panels (i)–(iv), 1 mm for the inset of the panel. Reproduced from [242]. CC BY 4.0.

to use it for numerous applications. DLP fabrication can address many of these limitations while providing a faster and more precise manufacturing strategy. Microwells are amongst the commonly used 2.5D structures. Both direct and indirect methods are employed for microwell array fabrication, indirect fabrication methods being more popular. Direct fabrication technique for preparing microwell arrays was demonstrated by Moussus for producing assays for root imaging. Tapering microwells with a larger diameter of 1.6 mm attached to a 28 mm long growth channel were fabricated by layer-by-layer DLP printing. Surface roughness was not a deciding parameter in the test's success, direct 3D printing was a preferred choice of fabrication [243]. Chen *et al* utilized layer-by-layer fabrication to produce positive molds, which were later templated onto PDMS to form microwell arrays [244]. Luan *et al* also preferred an indirect method to fabricate 75 μm deep microwells with 200 μm diameter onto PDMS. 3D printed masters provide a smoother surface finish, which provides better adhesion of cells [245].

Micropillars belong to a family of high aspect ratio structures that can be fabricated by repeatedly illuminating the same mask image until bristles of the desired size are obtained.

Such structures find applications in surface modification, tissue engineering, and microfluidics. DLP 3D printing is a popular choice for fabricating these structures. Due to the high aspect ratio, a layer-by-layer approach or CLIP printing is used for the fabrication of such structures. Tirado *et al* used layer-by-layer DLP printing with optimized light exposure to print high aspect ratio micro pillars [246]. Such structures with appropriate placement density can show interesting properties. Kaur *et al* demonstrated super hydrophobicity by printing arrays of fused silica micropillars on a flat substrate. Although the hydrophobic nature of the dispersed fused silica particles provided intrinsic roughness which favored water repellency, it was primarily due to the micropillar geometry [247]. Similar micro bristle arrays are also known to showcase increased mechanical adhesion [248]. Lattice patterns that can adopt shapes such as stars, cylinders, or ellipses can be easily fabricated using DLP-based vat polymerization. Such high-precision lattice structures make great candidates for studying cellular responses [249].

4.4.4. Other bioinspired structures. Nature presents us with a variety of micropatterned surfaces with multifunctional abilities. Most of these surfaces can be reproduced using the current AM processes. DLP printing has the ability and the flexibility to achieve this with close precision and high resolution using a variety of multifunctional materials and practically on any substrate imaginable. Researchers have been investigating the use of ink jetting over the past few decades and have realized the amazing potential of biomimetic micropatterned surfaces for a variety of applications like superhydrophobicity, filtration, cellular adhesion, water collection, etc. Cactus-inspired needle-like structures capable of water collection have been realized using micro-CLIP printing. The high resolution offered by projection-based grayscale printing allows to replicate the biomimetic designs. It is possible to fabricate features such as micro-ridges on each spine which exhibit capillary effects to capture water vapor [250]. Similar work was conducted by Chen's research group where they demonstrated DLP printed cactus inspired surfaces with directional spines for water collection. The cactus spikes exhibit high water retention due to their unique geometry. Replication of these geometries is possible using microscopic DLP technology as shown in figure 10(a). Their work has opened up new avenues in environmentally friendly ways of water collection and transportation [251]. The realization of these structures is only possible because of the advancements in DLP printing. Ray *et al* demonstrated the antiwetting properties of patterned PVDF membranes. The desired micropatterning was obtained by utilizing DLP-printed microstructured arrays to imprint on the PVDF membrane. The micropatterns generated on the PVDF were a result of post-imprinting solvent evaporation and non-solvent induced phase separation, which enhanced the antiwetting properties of PVDF significantly [252]. Li *et al* 3D printed peristome-mimetic structures and used PDMS replicating which had micro 'saw-tooth' arrays. Liquid transport was achieved using self-directional oil and water transport in opposite direction without energy input [253]. This liquid separation is made possible by the differences in the surface tension of the two liquids as depicted in the schematic in figure 10(b). Yang *et al* have developed an immersed surface accumulation-based AM process which uses a light guide tool with an objective lens for continuous projection of 2D images. The light guide tool is submerged inside the vat, which can allow for the fabrication of micro features with 2.5 μm resolution on conformal macro surfaces. They demonstrated the fabrication of biomimetic egg-beater geometry using E-glass/MWCNT composites with potential application in oil–water separation as shown in figure 10(c) [254]. Exploiting the non-uniform curing, Kim *et al* demonstrated shrinkage-induced bending to fabricate mushroom-like microstructures that can act as liquid-repellent surfaces. Micropillars were fabricated using a layer-by-layer process. To introduce mushroom like architecture, mechanical bending was introduced in the top layer by light intensity gradient. These structures could achieve omniphobicity without the need for additional chemical treatments [255]. As shown in figure 10(d), the water droplets tend to stay above the mushroom like structures by the virtue of surface tension preventing the wetting of the surface.

5. Conclusion and future directions

Nature has evolved over millions of years to develop functional micropatterned surfaces that showcase various interesting properties and functions. AM processes like inkjet printing and micro DLP printing have gained considerable attention in the past two decades for their low cost, high throughput, and high resilience. Another primary advantage of these processes is their ability to fabricate complex structures with relative ease whilst at times, mimicking the natural process. Recent developments have demonstrated more sustainable ways of fabricating as well as functionalizing micropatterned surfaces. The ability of rapid and large area-controlled solidification in response to UV light has made DLP a promising technology for microfabrication. As DLP printing uses focusing lenses to project the pattern on the vat containing resin, it is advantageous for feature scalability. DLP printing can fabricate stimuli-responsive microstructures, which has bolstered its place in 4D printed microstructures. Inkjet printing has complimented DLP printing by offering the ability to deploy material at predefined locations with extreme precision. Its ability to inherently deploy a variety of materials at precise locations has afforded its use in programmable and selective functionalization of the surfaces. This has made it a popular choice, especially in biomedical and drug testing applications. Inkjet printing was also seen as a very popular choice for microlens fabrication. The ability to tune the optical properties of microlenses by manipulating the surface energy of the substrate is being increasingly exploited for a variety of applications in optics, photonics, and biomedical research.

The reviewed literature underscores the significance of the choice of manufacturing process to specific applications. While achieving microfeatures is possible agnostic to the manufacturing process, certain methods offer distinct advantages

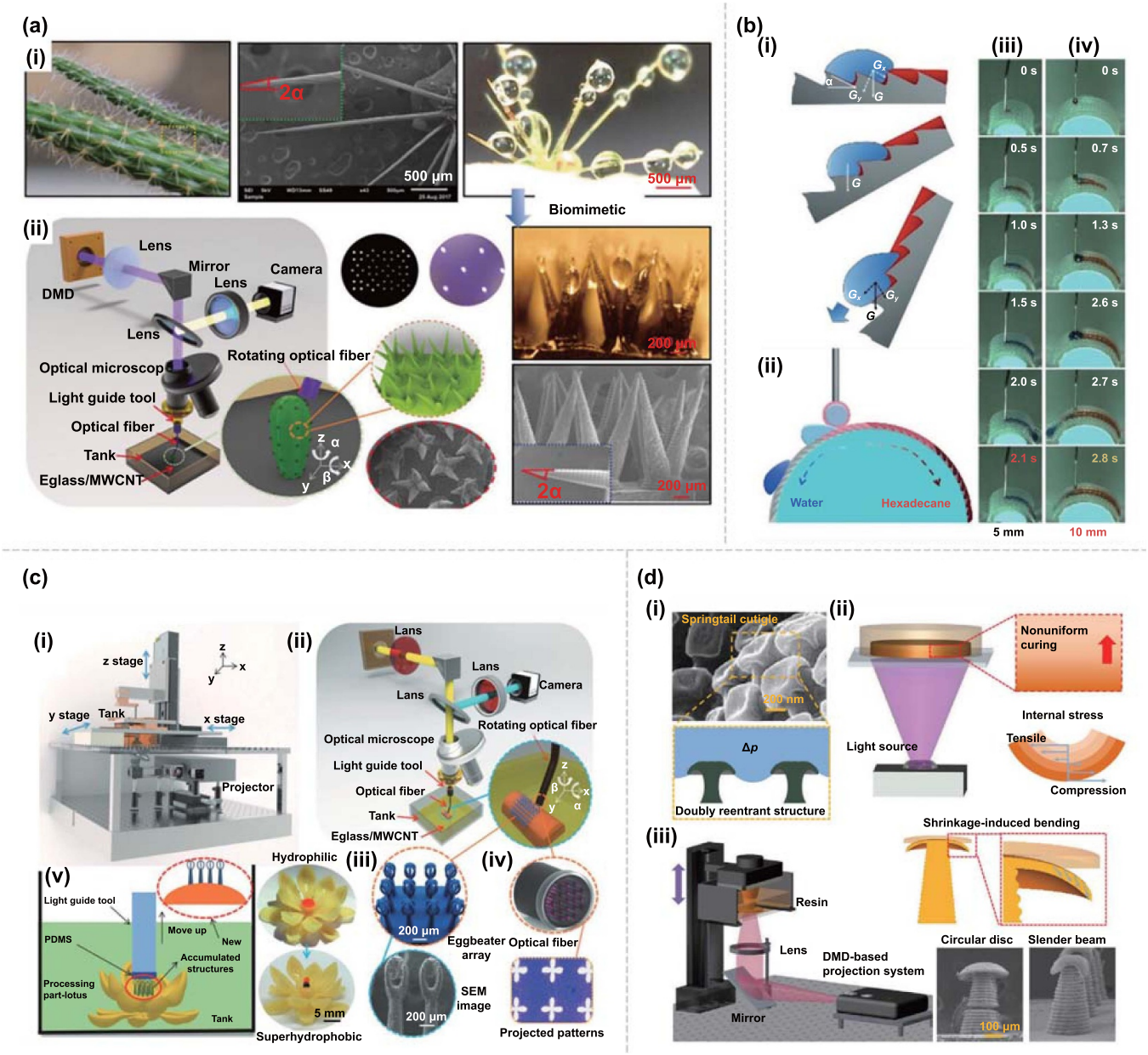

Figure 10. Nature inspired patterns. (a) Water collection using bio-inspired structures (i) Cactus covered with spines inspiring water collection mechanisms, (ii) DLP printed surface mimicking cactus needles [251]. John Wiley & Sons. © 2017 WILEY-VCH Verlag GmbH & Co. KGaA, Weinheim. (b) Oil–water separation (i) Schematic demonstration of the water pinning and sliding process on a tilted peristome-mimetic surface. For a horizontally mounted plate, the component of gravity forces the water flow forward, but the energy barrier induced by the overhang stops the spreading. At a tilt angle of 30°, the overhangs step horizontally at the rare sides of micro-cavities. Above 30°, gravity forces water to slide down, while oil phase pins at the overhang, (ii) schematic of microliter scaled water-hexadecane separation process on the peristome-mimetic surface, (iii) and (iv) time-lapse images of separation process with the curvature having radii of 5 mm and 10 mm respectively [253]. John Wiley & Sons. © 2017 Wiley-VCH Verlag GmbH & Co. KGaA, Weinheim. (c) Printing nature-inspired superhydrophobic structures (i) Schematic diagram of the immersed surface accumulation based 3D printing (ISA-3D) process; (ii) the optical system in the ISA-3D printing process (insert shows the magnification of light guide tool and optical fiber in (iv) with projected 2D micro patterns); (iii) models and SEM image of the 3D-printed eggbeater arrays; and (v) an illustration of adding microscale eggbeater structure on the free form curve surface of a lotus flower model, which changes the surface from hydrophilic to super-hydrophobic by using a straight light guide tool [254]. John Wiley & Sons. © 2017 WILEY-VCH Verlag GmbH & Co. KGaA, Weinheim. (d) Concept and fabrication of shape-deformed reentrant structures by shrinkage-induced mechanical bending. (i) Scanning electron microscopy (SEM) and schematic images showing the doubly reentrant structure in a springtail cuticle. (ii) Schematic presenting the frontal photopolymerization (FPP) process, (iii) Schematic of the DLP 3D printing system and shrinkage caused by FPP. SEM image of the fabricated doubly reentrant structures. Reprinted with permission from [255]. Copyright (2021) American Chemical Society.

in attaining desired surface quality with minimal complexity. The reviewed literature has directed us toward the fact that DOD inkjet printing is a particularly suitable choice for fabricating self-aligning structures like MLAs. Inkjet printing proves advantageous due to its ability to govern the meniscus formation of microlenses through fluid surface tension, facilitating the production of high-quality microlenses with superior surface finish. The literature emphasizes the role of substrate coating in enhancing tunability and realizing diverse microlens shapes. Inkjet printing is particularly adept at applications requiring precise placement, such as tissue engineering.

Conversely, when it comes to realizing intricate 3D structures, digital light processing (DLP) printing excels. The studied proximity effect and voxel growth dynamics contribute to the feasibility of achieving complex structures. Temporal tunability is achievable through the use of stimuli-responsive resins in DLP printing. It is also important to note that DLP printing is limited by the resolution of light, enabling the realization of ultrafine features that may be challenging with material deposition techniques like inkjet printing. The literature also suggests that a hybrid approach, integrating both energy deposition and material deposition techniques, exhibits enhanced placement accuracy, particularly beneficial in tissue engineering applications. This comprehensive understanding of the strengths and limitations of different manufacturing processes guides informed choices based on the specific requirements of diverse applications.

Much effort has been directed towards the fabrication of functional micropatterned surfaces using various additives as well as conventional methods. Considering the advantages that micro DLP and inkjet systems provide, our efforts were directed toward studying the works concerning these processes in detail. Despite the relative maturity of both inkjet and DLP processes, they are still laden with challenges, especially at the micron scale.

1. Smaller features are extremely difficult to print as the diffraction of light from an illuminated pixel leads to energy distribution. In the case of larger features, this can be seen as advantageous, but in smaller features, it leads to part truncation [227]. This effect is believed to be caused due to oxygen inhibition but hasn't yet been quantified. Extreme printing resolution is, therefore, not possible using the current DLP systems. Micropattern packing density can showcase various characteristics. Precise control over the feature packing density is thus desired. Light spreading and dark field effects play a crucial role in determining the resolution of patterned microstructure arrays. Light from adjacent features bleeds into the neighboring pixels, giving rise to sporadic connections. This loss of feature resolution due to the closeness and influence of other features is termed as 'proximity effect'. Although this effect is known to occur, it still lacks quantification and has thus hindered the efforts towards printing high-resolution micropatterns. Current simulation models based on the basic understanding of photopolymerization kinetics and light propagation are not quite relevant at the micron scale. As complex light-matter interactions are involved, data-driven models should be preferred over physics-based models. Collecting voxel growth data will provide a better understanding of the actual process. As observing the process in situ is challenging, appropriate tools need to be developed. The resolution of the DLP process is limited by the pixel size, using controlled vibration-assisted projection can help realize sub-pixel resolution.
2. Although inkjet printing is relatively mature, it comes with its own set of challenges. Although individual printable functional materials have shown significant performance, a significant breakthrough is still needed to implement multifunctional materials. The jetting parameters need to be tuned precisely according to the material, which makes it laborious, less reliable, and difficult to replicate. Although data-driven models have been used to study the jetting behavior, parameter optimization based on these models has not been successfully achieved [102, 256]. Droplets landing on the substrate tend to merge at higher spatial density. Although the use of evaporating solvents has helped reduce this effect, its reliability is still questionable. The relatively poor resolution of inkjet printing is limiting its scope in micropattern array fabrication. To address this issue, more reliable inkjet process with sub-micron resolution jetting hardware and a better understanding of ink rheology needs to be developed.
3. Furthermore, both the fabrication techniques discussed in this review exhibit dynamic and non-linear characteristics. Hindsight observations cannot provide accurate and comprehensive information regarding the process. Therefore, better observation tools capable of in-situ monitoring and extracting relevant and high-quality data need to be developed. Existing simulations often rely on a theoretical understanding of the process, neglecting the intricate interplay of various factors affected by the ambient conditions. To advance micropattern fabrication, it is imperative to develop enhanced simulation models incorporating physics-informed principles and observational data. Predictive models based on the collected process data and active feedback will provide a more reliable and efficient approach to fabricating micropatterns. By bridging the gap between theory and observation, these models can help in process optimization, thus resulting in high precision production of intricate micropatterns.

Another critical aspect of micropatterning is the utilization of data-driven techniques for pattern design [257]. Artificial intelligence has proven instrumental in engineering innovative hierarchical structures and multiscale surfaces with controlled functionality [258, 259]. In conjunction with the existing literature, substantial advancements have been made by integrating machine learning and data-driven methodologies to comprehend and achieve diverse micropatterns. Machine learning serves as a robust tool for steering the design process toward specific functionalities, playing a significant role in pattern design, optimization, and modulation. It has found application in pattern design and optimization, as well as design modulation. However, the scope of this work prevents a thorough examination of these complexities. The major focus here is on

studying and grasping the most recent advances in microfabrication methods and their many applications. Given the limited scope, this work will not delve into the finer details of machine learning's role in optimizing micropattern arrays. To fully explore and understand the improvement of micropattern arrays, we need a detailed examination specifically focused on design optimization. This dedicated exploration is crucial for discussing the various techniques used to enhance the design and functionality of micropatterned structures. Such a focused review would shed light on the dynamic interplay between machine learning and micropattern design, unveiling further dimensions of innovation in the field.

Despite these process challenges, in a positive perspective, both inkjet printing and micro DLP printing are promising pathways towards realizing low-cost and highly reliable micropatterned multifunctional surfaces. These cutting-edge technologies have the potential to revolutionize the production of functional micropatterns, making them more accessible, effective, and reliable for a wide variety of applications. The reviewed literature suggests that process improvement is only possible by more robust understanding of the underlying mechanisms. This understanding is essential for unlocking the true potential of inkjet and microSLA technologies in microfabrication. We can anticipate significant advances and ground-breaking developments in microscale production by delving into the specifics of these procedures. This study highlights that understanding the fundamental concepts is the key to fostering meaningful advancement in the fields of science and innovation.

Acknowledgments

The authors would like to gratefully acknowledge the support from the National Science Foundation (NSF) through Grants ECCS-2111056 and CMMI-1846863.

ORCID iD

Chi Zhou https://orcid.org/0000-0001-7230-3754

References

[1] Arzt E, Quan H C, Mcmeeking R M and Hensel R 2021 Functional surface microstructures inspired by nature–From adhesion and wetting principles to sustainable new devices *Prog. Mater. Sci.* **120** 100823
[2] Jin H C, Tian L M, Bing W, Zhao J and Ren L Q 2022 Bioinspired marine antifouling coatings: status, prospects, and future *Prog. Mater. Sci.* **124** 100889
[3] Bandyopadhyay A, Traxel K D and Bose S 2021 Nature-inspired materials and structures using 3D printing *Mater. Sci. Eng.* R **145** 100609
[4] Damodaran V B and Murthy N S 2016 Bio-inspired strategies for designing antifouling biomaterials *Biomater. Res.* **20** s40824–016–0064–4
[5] Wang F H, Huang H, Yaniv K, Kushmaro A and Bernstein R 2022 Self-assembly of adjustable micropatterned graphene oxide and reduced graphene oxide on porous polymeric surfaces *Adv. Mater. Interfaces* **9** 2102429
[6] Yan X X, Bethers B, Chen H X, Xiao S Q, Lin S, Tran B, Jiang L M and Yang Y 2021 Recent advancements in biomimetic 3D printing materials with enhanced mechanical properties *Front. Mater.* **8** 518886
[7] Liu M J, Wang S T and Jiang L 2017 Nature-inspired superwettability systems *Nat. Rev. Mater.* **2** 17036
[8] Zhang D J, Cheng Z J, Kang H J, Yu J X, Liu Y Y and Jiang L 2018 A smart superwetting surface with responsivity in both surface chemistry and microstructure *Angew. Chem.* **130** 3763–7
[9] Nørgaard T and Dacke M 2010 Fog-basking behaviour and water collection efficiency in Namib Desert Darkling beetles *Front. Zool* **7** 23
[10] Dean B and Bhushan B 2010 Shark-skin surfaces for fluid-drag reduction in turbulent flow: a review *Phil. Trans. R. Soc.* A **368** 4775–806
[11] Rostami S and Garipcan B 2022 Evolution of antibacterial and antibiofouling properties of sharkskin-patterned surfaces *Surf. Innov.* **10** 165–90
[12] Cutkosky M R and Kim S 2009 Design and fabrication of multi-material structures for bioinspired robots *Phil. Trans. R. Soc.* A **367** 1799–813
[13] Xiang Y L, Huang S L, Huang T Y, Dong A, Cao D, Li H Y, Xue Y H, Lv P Y and Duan H L 2020 Superrepellency of underwater hierarchical structures on *Salvinia* leaf *Proc. Natl Acad. Sci. USA* **117** 2282–7
[14] Liu X J, Gu H C, Ding H B, Du X, Wei M X, Chen Q and Gu Z Z 2020 3D bioinspired microstructures for switchable repellency in both air and liquid *Adv. Sci.* **7** 2000878
[15] Dayan C B, Chun S, Krishna-subbaiah N, Drotlef D M, Akolpoglu M B and Sitti M 2021 3D printing of elastomeric bioinspired complex adhesive microstructures *Adv. Mater.* **33** 2103826
[16] Chen Z, Chun S, Krishna-subbaiah N, Drotlef D M, Akolpoglu M B and Sitti M 2018 Additive manufacturing of honeybee-inspired microneedle for easy skin insertion and difficult removal *ACS Appl. Mater. Interfaces* **10** 29338–46
[17] Kovacs G T A, Maluf N I and Petersen K E 1998 Bulk micromachining of silicon *Proc. IEEE* **86** 1536–51
[18] Xie J, Zhuo Y W and Tan T W 2011 Experimental study on fabrication and evaluation of micro pyramid-structured silicon surface using a V-tip of diamond grinding wheel *Precis. Eng.* **35** 173–82
[19] Moon S D, Lee N and Kang S 2003 Fabrication of a microlens array using micro-compression molding with an electroformed mold insert *J. Micromech. Microeng.* **13** 98–103
[20] Zhu T F, Fu J, Wang W, Wen F, Zhang J W, Bu R N, Ma M T and Wang H X 2017 Fabrication of diamond microlenses by chemical reflow method *Opt. Express* **25** 1185–92
[21] Albero J, Nieradko L, Gorecki C, Ottevaere H, Gomez V, Thienpont H, Pietarinen J, Päivänranta B and Passilly N 2009 Fabrication of spherical microlenses by a combination of isotropic wet etching of silicon and molding techniques *Opt. Express* **17** 6283–92
[22] Wu M H, Park C and Whitesides G M 2002 Fabrication of arrays of microlenses with controlled profiles using gray-scale microlens projection photolithography *Langmuir* **18** 9312–8
[23] Gao P, Liang Z Q, Wang X B, Zhou T F, Xie J Q, Li S D and Shen W H 2018 Fabrication of a micro-lens array mold by micro ball end-milling and its hot embossing *Micromachines* **9** 96

[24] Matsuo S, Juodkazis S and Misawa H 2005 Femtosecond laser microfabrication of periodic structures using a microlens array *Appl. Phys.* A **80** 683–5

[25] Hu H, Tian H M, Shao J Y, Ding Y C, Jiang C B and Liu H Z 2014 Fabrication of bifocal microlens arrays based on controlled electrohydrodynamic reflowing of pre-patterned polymer *J. Micromech. Microeng.* **24** 095027

[26] Maghsoudi K, Vazirinasab E, Momen G and Jafari R 2020 Advances in the fabrication of superhydrophobic polymeric surfaces by polymer molding processes *Ind. Eng. Chem. Res.* **59** 9343–63

[27] Sowade E, Polomoshnov M, Willert A and Baumann R R 2019 Toward 3D-printed electronics: inkjet-printed vertical metal wire interconnects and screen-printed batteries *Adv. Eng. Mater.* **21** 1900568

[28] Xie D, Zhang H H, Shu X Y and Xiao J F 2012 Fabrication of polymer micro-lens array with pneumatically diaphragm-driven drop-on-demand inkjet technology *Opt. Express* **20** 15186–95

[29] Alamán J, Alicante R, Peña J and Sánchez-Somolinos C 2016 Inkjet printing of functional materials for optical and photonic applications *Materials* **9** 910

[30] Kawale S S, Jang I, Farandos N M and Kelsall G H 2022 Inkjet 3D-printing of functional layers of solid oxide electrochemical reactors: a review *React. Chem. Eng.* **7** 1692–712

[31] Su W J, Cook B S, Fang Y N and Tentzeris M M 2016 Fully inkjet-printed microfluidics: a solution to low-cost rapid three-dimensional microfluidics fabrication with numerous electrical and sensing applications *Sci. Rep.* **6** 35111

[32] Zhang Q S, Schambach M, Schlisske S, Jin Q H, Mertens A, Rainer C, Hernandez-Sosa G, Heizmann M and Lemmer U 2022 Fabrication of microlens arrays with high quality and high fill factor by inkjet printing *Adv. Opt. Mater.* **10** 2200677

[33] Luo Y, Wang L, Ding Y C, Wei H F, Hao X Q, Wang D D, Dai Y and Shi J F 2013 Direct fabrication of microlens arrays with high numerical aperture by ink-jetting on nanotextured surface *Appl. Surf. Sci.* **279** 36–40

[34] da Costa T H and Choi J W 2020 Low-cost and customizable inkjet printing for microelectrodes fabrication *Micro Nano Syst. Lett.* **8** 2

[35] Grubb P M, Subbaraman H, Park S, Akinwande D and Chen R T 2017 Inkjet printing of high performance transistors with micron order chemically set gaps *Sci. Rep.* **7** 1202

[36] Yang Y J, Kim H C, Sajid M, Kim S W, Aziz S, Choi Y S and Choi K H 2018 Drop-on-demand electrohydrodynamic printing of high resolution conductive micro patterns for MEMS repairing *Int. J. Precis. Eng. Manuf.* **19** 811–9

[37] Onses M S, Sutanto E, Ferreira P M, Alleyne A G and Rogers J A 2015 Mechanisms, capabilities, and applications of high-resolution electrohydrodynamic jet printing *Small* **11** 4237–66

[38] Barton K, Mishra S, Alleyne A, Ferreira P and Rogers J 2011 Control of high-resolution electrohydrodynamic jet printing *Control Eng. Pract.* **19** 1266–73

[39] Mishra S, Barton K L, Alleyne A G, Ferreira P M and Rogers J A 2010 High-speed and drop-on-demand printing with a pulsed electrohydrodynamic jet *J. Micromech. Microeng.* **20** 095026

[40] Han Y W, Wei C and Dong J Y 2014 Super-resolution electrohydrodynamic (EHD) 3D printing of micro-structures using phase-change inks *Manuf. Lett.* **2** 96–99

[41] OPTOMEC 2014 Aerosol Jet ® printed electronics overview

[42] Umrani A 2015 *Fabrication of Micro Pillar Arrays via Aerosol Jet Printing* (Rochester Institute of Technology)

[43] Cooper C and Hughes B 2020 Aerosol jet printing of electronics: an enabling technology for wearable devices *Proc. of 2020 Pan Pacific Microelectronics Symp. (Pan Pacific)* (IEEE)

[44] Yan C Y, Jiang P, Jia X and Wang X L 2020 3D printing of bioinspired textured surfaces with superamphiphobicity *Nanoscale* **12** 2924–38

[45] Yang Q L, Zhong W Z, Xu L, Li H J, Yan Q Y, She Y B and Yang G S 2021 Recent progress of 3D-printed microneedles for transdermal drug delivery *Int. J. Pharm.* **593** 120106

[46] Emami M M and Rosen D W 2018 An improved vat photopolymerization cure model demonstrates photobleaching effects *Proc. 29th Annual Int. Solid Freeform Fabrication Symp.—An Additive Manufacturing Conf.* (*Austin, TX*)

[47] Emami M M and Rosen D W 2020 Modeling of light field effect in deep vat polymerization for grayscale lithography application *Addit. Manuf.* **36** 101595

[48] Emami M M, Jamshidian M and Rosen D W 2021 Multiphysics modeling and experiments of grayscale photopolymerization with application to microlens fabrication *J. Manuf. Sci. Eng.* **143** 091005

[49] Zhang J M, Hu P, Wang S, Tao J and Gou M L 2019 Digital light processing based three-dimensional printing for medical applications *Int. J. Bioprint.* **6** 242

[50] Doraiswamy A, Jin C, Narayan R, Mageswaran P, Mente P, Modi R, Auyeung R, Chrisey D, Ovsianikov A and Chichkov B 2006 Two photon induced polymerization of organic–inorganic hybrid biomaterials for microstructured medical devices *Acta Biomater.* **2** 267–75

[51] Doraiswamy A, Ovsianikov A, Gittard S, Monteiro-Riviere N, Crombez R, Montalvo E, Shen W D, Chichkov B and Narayan R 2010 Fabrication of microneedles using two photon polymerization for transdermal delivery of nanomaterials *J. Nanosci. Nanotechnol.* **10** 6305–12

[52] Burmeister F, Zeitner U D, Nolte S and Tünnermann A 2012 High numerical aperture hybrid optics for two-photon polymerization *Opt. Express* **20** 7994–8005

[53] Jonušauskas L, Baravykas T, Andrijec D, Gadišauskas T and Purlys V 2019 Stitchless support-free 3D printing of free-form micromechanical structures with feature size on-demand *Sci. Rep.* **9** 17533

[54] Hou T X, Zheng C, Bai S, Ma Q, Bridges D, Hu A M and Duley W W 2015 Fabrication, characterization, and applications of microlenses *Appl. Opt.* **54** 7366–76

[55] Sitti M 2003. High aspect ratio polymer micro/nano-structure manufacturing using nanoembossing, nanomolding and directed self-assembly *Proc. 2003 IEEE/ASME Int. Conf. on Advanced Intelligent Mechatronics (AIM 2003)* (IEEE) (https://doi.org/10.1109/tuffc.2003.1193617)

[56] Xu M, Zhou Z W, Wang Z and Lu H B 2020 Self-assembled microlens array with controllable focal length formed on a selective wetting surface *ACS Appl. Mater. Interfaces* **12** 7826–32

[57] Lian Z J, Hung S Y, Shen M H and Yang H 2014 Rapid fabrication of semiellipsoid microlens using thermal reflow with two different photoresists *Microelectron. Eng.* **115** 46–50

[58] Di S and Du R X 2009 The controlling of microlens contour by adjusting developing time in the thermal reflow method *Proc. SPIE* **7381** 73811D

[59] Roy E, Voisin B, Gravel J F, Peytavi R, Boudreau D and Veres T 2009 Microlens array fabrication by enhanced thermal reflow process: towards efficient collection of fluorescence light from microarrays *Microelectron. Eng.* **86** 2255–61

[60] Yang H, Chao C K, Wei M K and Lin C P 2004 High fill-factor microlens array mold insert fabrication using a thermal reflow process *J. Micromech. Microeng.* **14** 1197–204

[61] Zhang Z Y, Yan J W and Kuriyagawa T 2019 Manufacturing technologies toward extreme precision *Int. J. Extrem. Manuf.* **1** 022001

[62] Lakshminarayanan S 2018 Micro/nano patterning on polymers using soft lithography technique *Micro/Nanolithography-A Heuristic Aspect on the Enduring Technology* ed J Thirumalai (IntechOpen)

[63] Qian T C and Wang Y X 2010 Micro/nano-fabrication technologies for cell biology *Med. Biol. Eng. Comput.* **48** 1023–32

[64] Hartensveld M 2018 *Optimization of Dry and Wet GaN Etching to Form High Aspect Ratio Nanowires* (Rochester Institute of Technology)

[65] Samsung 2022 Learn display 47 Etching (available at: http://global.samsungdisplay.com/29533/)

[66] Bibber D 2012 Secrets of success in micro molding (available at: www.ptonline.com/articles/secrets-of-success-in-micro-molding)

[67] Heckele M and Schomburg W 2003 Review on micro molding of thermoplastic polymers *J. Micromech. Microeng.* **14** R1

[68] Quirk M and Serda J 2001 *Semiconductor Manufacturing Technology* (Prentice Hall)

[69] Wu J and Gu M 2011 Microfluidic sensing: state of the art fabrication and detection techniques *J. Biomed. Opt.* **16** 080901

[70] Magazine R, Van Bochove B, Borandeh S and Seppälä J 2022 3D inkjet-printing of photo-crosslinkable resins for microlens fabrication *Addit. Manuf.* **50** 102534

[71] Negro A, Cherbuin T and Lutolf M P 2018 3D inkjet printing of complex, cell-laden hydrogel structures *Sci. Rep.* **8** 17099

[72] Rao C H, Avinash K, Varaprasad B K S V L and Goel S 2022 A review on printed electronics with digital 3D printing: fabrication techniques, materials, challenges and future opportunities *J. Electron. Mater.* **51** 2747–65

[73] Gao D J and Zhou J G 2019 Designs and applications of electrohydrodynamic 3D printing *Int. J. Bioprint.* **5** 172

[74] Zhang G M, Qian L, Zhao J W, Zhou H F and Lan H B 2018 High-resolution electric-field-driven jet 3D printing and applications *3D Printing* ed D Cvetković (IntechOpen)

[75] De Gans B J, Duineveld P C and Schubert U S 2004 Inkjet printing of polymers: state of the art and future developments *Adv. Mater.* **16** 203–13

[76] Luo Y 2005 *Functional Nanostructures by Ordered Porous Templates* (Universitäts- und Landesbibliothek Sachsen-Anhalt)

[77] Krainer S, Smit C and Hirn U 2019 The effect of viscosity and surface tension on inkjet printed picoliter dots *RSC Adv.* **9** 31708–19

[78] Oktavianty O, Haruyama S and Ishii Y 2022 Enhancing droplet quality of edible ink in single and multi-drop methods by optimization the waveform design of DoD inkjet printer *Processes* **10** 91

[79] Tofan T, Kruggel-Emden H, Turla V and Jasevičius R 2021 Numerical modeling of the motion and interaction of a droplet of an inkjet printing process with a flat surface *App. Sci.* **11** 527

[80] Cooley P W, Wallace D B and Antohe B V 2001 Applications of ink-jet printing technology to BioMEMS and microfluidic systems *Proc. SPIE* **4560** 177–188

[81] Li J, Rossignol F and Macdonald J 2015 Inkjet printing for biosensor fabrication: combining chemistry and technology for advanced manufacturing *Lab Chip* **15** 2538–58

[82] Kim S, Choi J H, Sohn D K and Ko H S 2022 The effect of ink supply pressure on piezoelectric inkjet *Micromachines* **13** 615

[83] van der Bos A, Van Der Meulen M J, Driessen T, Van Den Berg M, Reinten H, Wijshoff H, Versluis M and Lohse D 2014 Velocity profile inside piezoacoustic inkjet droplets in flight: comparison between experiment and numerical simulation *Phys. Rev. Appl.* **1** 014004

[84] Xu L, Zhang W W and Nagel S R 2005 Drop splashing on a dry smooth surface *Phys. Rev. Lett.* **94** 184505

[85] Furlani E P, Price B G, Hawkins H and Lopez A G 2006 Thermally induced Marangoni instability of liquid microjets with application to continuous inkjet printing *Proc. NSTI Nanotechnology Conf.* (Nano Science and Technology Institute) (https://doi.org/10.1103/PhysRevE.73.061919)

[86] Shah M A, Lee D G, Lee B Y, Kim N W, An H and Hur S 2020 Actuating voltage waveform optimization of piezoelectric inkjet printhead for suppression of residual vibrations *Micromachines* **11** 900

[87] Kwon K S 2009 Waveform design methods for piezo inkjet dispensers based on measured meniscus motion *J. Microelectromech. Syst.* **18** 1118–25

[88] Bogy D B and Talke F E 1984 Experimental and theoretical study of wave propagation phenomena in drop-on-demand ink jet devices *IBM J. Res. Dev.* **28** 314–21

[89] Effects P W and Effects P A 1999 *Drive Waveform Effects on Ink-Jet Device Performance* (MicroFab Technologies Inc.) pp 99–103

[90] Szczech J B, Megaridis C M, Gamota D R and Zhang J 2002 Fine-line conductor manufacturing using drop-on demand PZT printing technology *IEEE Trans. Electron. Packag. Manuf* **25** 26–33

[91] Hu Z J, Li S J, Yang F, Lin X J, Pan S Q, Huang X F and Xu J R 2021 Formation and elimination of satellite droplets during monodisperse droplet generation by using piezoelectric method *Micromachines* **12** 921

[92] Riefler N and Wriedt T 2008 Generation of monodisperse micron-sized droplets using free adjustable signals *Part. Part. Syst. Charact.* **25** 176–82

[93] Dong H M, Carr W W and Morris J F 2006 An experimental study of drop-on-demand drop formation *Phys. Fluids* **18** 072102

[94] Fraters A, Jeurissen R, Van Den Berg M, Reinten H, Wijshoff H, Lohse D, Versluis M and Segers T 2020 Secondary tail formation and breakup in piezoacoustic inkjet printing: femtoliter droplets captured in flight *Phys. Rev. Appl.* **13** 024075

[95] Herran C L and Huang Y 2012 Alginate microsphere fabrication using bipolar wave-based drop-on-demand jetting *J. Manuf. Process.* **14** 98–106

[96] Herran C L and Coutris N 2013 Drop-on-demand for aqueous solutions of sodium alginate *Exp. Fluids* **54** 1548

[97] Shin P, Sung J and Lee M H 2011 Control of droplet formation for low viscosity fluid by double waveforms applied to a piezoelectric inkjet nozzle *Microelectron. Reliab.* **51** 797–804

[98] Kim B H, Kim S I, Lee J C, Shin S J and Kim S J 2012 Dynamic characteristics of a piezoelectric driven inkjet printhead fabricated using MEMS technology *Sens. Actuators* A **173** 244–53

[99] Morita N, Hamazaki T and Ishiyama T 2016 Observation on satellite behavior by double-pulse driving for high-speed inkjet *J. Imaging Sci. Technol.* **60** 40503

[100] Verkouteren R M and Verkouteren J R 2011 Inkjet metrology II: resolved effects of ejection frequency, fluidic pressure, and droplet number on reproducible drop-on-demand dispensing *Langmuir* **27** 9644–53

[101] Tsai M H and Hwang W S 2008 Effects of pulse voltage on the droplet formation of alcohol and ethylene glycol in a piezoelectric inkjet printing process with bipolar pulse *Mater. Trans.* **49** 331–8
[102] Huang J D, Segura L J, Wang T J, Zhao G L, Sun H Y and Zhou C 2020 Unsupervised learning for the droplet evolution prediction and process dynamics understanding in inkjet printing *Addit. Manuf.* **35** 101197
[103] Hill T Y 2019 *Understanding Drop-on-Demand Inkjet Process Characteristics in the Application of Printing Micro Solid Oxide Fuel Cells* (Wright State University)
[104] Lee A, Sudau K, Ahn K H, Lee S J and Willenbacher N 2012 Optimization of experimental parameters to suppress nozzle clogging in inkjet printing *Ind. Eng. Chem. Res.* **51** 13195–204
[105] Derby B 2010 Inkjet printing of functional and structural materials: fluid property requirements, feature stability, and resolution *Annu. Rev. Mater. Res.* **40** 395–414
[106] Tanner L H 1979 The spreading of silicone oil drops on horizontal surfaces *J. Phys. D: Appl. Phys.* **12** 1473–84
[107] Yarin A L 2006 Drop impact dynamics: splashing, spreading, receding, bouncing *Annu. Rev. Fluid Mech.* **38** 159–92
[108] Wang F J, Yang L, Wang L B, Zhu Y and Fang T G 2019 Maximum spread of droplet impacting onto solid surfaces with different wettabilities: adopting a rim–lamella shape *Langmuir* **35** 3204–14
[109] Toivakka M 2003 Numerical investigation of droplet impact spreading in spray coating of paper *Proceedings 2003 Advanced Coating Fundamentals Symp. Proc.*
[110] Li R, Ashgriz N and Chandra S 2010 Maximum spread of droplet on solid surface: low Reynolds and Weber numbers *J. Fluids Eng.* **132** 061302
[111] Yan K, Li J A, Pan L J and Shi Y 2020 Inkjet printing for flexible and wearable electronics *APL Mater.* **8** 120705
[112] Jang D, Kim D and Moon J 2009 Influence of fluid physical properties on ink-jet printability *Langmuir* **25** 2629–35
[113] Castrejón-Pita J R, Morrison N F, Harlen O G, Martin G D and Hutchings I M 2011 Experiments and Lagrangian simulations on the formation of droplets in drop-on-demand mode *Phys. Rev.* E **83** 036306
[114] Liu Y Y and Derby B 2019 Experimental study of the parameters for stable drop-on-demand inkjet performance *Phys. Fluids* **31** 032004
[115] Anyfantakis M, Geng Z, Morel M, Rudiuk S and Baigl D 2015 Modulation of the coffee-ring effect in particle/surfactant mixtures: the importance of particle–interface interactions *Langmuir* **31** 4113–20
[116] Gao M, Li L H and Song Y L 2017 Inkjet printing wearable electronic devices *J. Mater. Chem.* C **5** 2971–93
[117] Yamanaka K, Oakamoto H, Kidou H and Kudo T 1986 Peroxotungstic acid coated films for electrochromic display devices *Jpn. J. Appl. Phys.* **25** 1420
[118] Cheng Z Y, Xing R B, Hou Z Y, Huang S S and Lin J 2010 Patterning of light-emitting YVO4:Eu^{3+} thin films via inkjet printing *J. Phys. Chem.* C **114** 9883–8
[119] Yuan W, Li L H, Lee W B and Chan C Y 2018 Fabrication of microlens array and its application: a review *Chin. J. Mech. Eng.* **31** 16
[120] MacFarlane D L, Narayan V, Tatum J A, Cox W R, Chen T and Hayes D J 1994 Microjet fabrication of microlens arrays *IEEE Photonics Technol. Lett.* **6** 1112–4
[121] Ishii Y, Koike S, Arai Y and Ando Y 2000 Ink-jet fabrication of polymer microlens for optical-I/O chip packaging *Jpn. J. Appl. Phys.* **39** 1490
[122] Voigt A, Ostrzinski U, Pfeiffer K, Kim J Y, Fakhfouri V, Brugger J and Gruetzner G 2011 New inks for the direct drop-on-demand fabrication of polymer lenses *Microelectron. Eng.* **88** 2174–9
[123] Biehl S, Danzebrink R, Oliveira P and Aegerter M A 1998 Refractive microlens fabrication by ink-jet process *J. Sol-Gel Sci. Technol.* **13** 177–82
[124] Parry E, Bolis S, Castrejón-Pita A, Elston S J and Morris S M 2017 Drop-on-demand inkjet printing of liquid crystals and the fabrication of tuneable microlens arrays *European Conf. on Liquid Crystals 2017* (*Moscow, Russia*)
[125] Parry E, Bolis S, Elston S J, Castrejón-Pita A A and Morris S M 2018 Drop-on-demand inkjet printing of thermally tunable liquid crystal microlenses *Adv. Eng. Mater.* **20** 1700774
[126] Kamal W, Lin J D, Elston S J, Ali T, Castrejón-Pita A A and Morris S M 2020 Electrically tunable printed bifocal liquid crystal microlens arrays *Adv. Mater. Interfaces* **7** 2000578
[127] Sanchez E A, Waldmann M and Arnold C B 2011 Chalcogenide glass microlenses by inkjet printing *Appl. Opt.* **50** 1974–8
[128] Fakhfouri V, Cantale N, Mermoud G, Kim J Y, Boiko D, Charbon E, Martinoli A and Brugger J 2008 Inkjet printing of SU-8 for polymer-based MEMS a case study for microlenses *Proc. IEEE 21st Int. Conf. on Micro Electro Mechanical Systems* (IEEE)
[129] Deegan R D, Bakajin O, Dupont T F, Huber G, Nagel S R and Witten T A 1997 Capillary flow as the cause of ring stains from dried liquid drops *Nature* **389** 827–9
[130] Xia Y J and Friend R H 2007 Nonlithographic patterning through inkjet printing via holes *Appl. Phys. Lett.* **90** 253513
[131] Chen F C, Lu J P and Huang W K 2009 Using ink-jet printing and coffee ring effect to fabricate refractive microlens arrays *IEEE Photonics Technol. Lett.* **21** 648–50
[132] Alamán J, María López-Villuendas A, López-Valdeolivas M, Arroyo M P, Andrés N and Sánchez-Somolinos C 2020 Facile fabrication of microlenses with controlled geometrical characteristics by inkjet printing on nanostructured surfaces prepared by combustion chemical vapour deposition *Appl. Surf. Sci.* **510** 145422
[133] Wang D Y, Liu Z Y, Wang H Z, Li M X, Guo L J and Zhang C 2023 Structural color generation: from layered thin films to optical metasurfaces *Nanophotonics* **12** 1019–81
[134] Cox W R, Chen T, Ussery D, Hayes D J, Tatum J A and Macfarlane D L 1996 Microjetted lenslet triplet fibers *Opt. Commun.* **123** 492–6
[135] Tien C H, Hung C H and Yu T H 2009 Microlens arrays by direct-writing inkjet print for LCD backlighting applications *J. Disp. Technol.* **5** 147–51
[136] Kim J Y, Brauer N B, Fakhfouri V, Boiko D L, Charbon E, Grutzner G and Brugger J 2011 Hybrid polymer microlens arrays with high numerical apertures fabricated using simple ink-jet printing technique *Opt. Mater. Express* **1** 259–69
[137] Jacot-Descombes L, Cadarso V J, Schleunitz A, Grützner S, Klein J J, Brugger J, Schift H and Grützner G 2015 Organic-inorganic-hybrid-polymer microlens arrays with tailored optical characteristics and multi-focal properties *Opt. Express* **23** 25365–76
[138] Li J, Wang W J, Mei X S, Hou D X, Pan A F, Liu B and Cui J L 2020 Fabrication of artificial compound eye with controllable field of view and improved imaging *ACS Appl. Mater. Interfaces* **12** 8870–8
[139] Goodling A E, Nagelberg S, Kolle M and Zarzar L D 2020 Tunable and responsive structural color from polymeric microstructured surfaces enabled by interference of totally internally reflected light *ACS Mater. Lett.* **2** 754–63
[140] Li L K *et al* 2021 Facile full-color printing with a single transparent ink *Sci. Adv.* **7** eabh1992
[141] Phillippi J A, Miller E, Weiss L, Huard J, Waggoner A and Campbell P 2008 Microenvironments engineered by inkjet bioprinting spatially direct adult stem cells toward

muscle-and bone-like subpopulations *Stem Cells* **26** 127–34
[142] Turcu F, Tratsk-Nitz K, Thanos S, Schuhmann W and Heiduschka P 2003 Ink-jet printing for micropattern generation of laminin for neuronal adhesion *J. Neurosci. Methods* **131** 141–8
[143] Roth E A, Xu T, Das M, Gregory C, Hickman J J and Boland T 2004 Inkjet printing for high-throughput cell patterning *Biomaterials* **25** 3707–15
[144] Liberski A R, Delaney J T Jr and Schubert U S 2011 'One cell− one well': a new approach to inkjet printing single cell microarrays *ACS Comb. Sci.* **13** 190–5
[145] Yusof A, Keegan H, Spillane C D, Sheils O M, Martin C M, O'leary J J, Zengerle R and Koltay P 2011 Inkjet-like printing of single-cells *Lab Chip* **11** 2447–54
[146] Fujita S, Onuki-Nagasaki R, Fukuda J, Enomoto J, Yamaguchi S and Miyake M 2013 Development of super-dense transfected cell microarrays generated by piezoelectric inkjet printing *Lab Chip* **13** 77–80
[147] Fujie T, Desii A, Ventrelli L, Mazzolai B and Mattoli V 2012 Inkjet printing of protein microarrays on freestanding polymeric nanofilms for spatio-selective cell culture environment *Biomed. Microdev.* **14** 1069–76
[148] Sun W Z, Taylor C S, Zhang Y, Gregory D A, Tomeh M A, Haycock J W, Smith P J, Wang F, Xia Q Y and Zhao X B 2021 Cell guidance on peptide micropatterned silk fibroin scaffolds *J. Colloid Interface Sci.* **603** 380–90
[149] Gantumur E, Kimura M, Taya M, Horie M, Nakamura M and Sakai S 2019 Inkjet micropatterning through horseradish peroxidase-mediated hydrogelation for controlled cell immobilization and microtissue fabrication *Biofabrication* **12** 011001
[150] Martinez-Rivas A, González-Quijano G, Proa-Coronado S, Séverac C and Dague E 2017 Methods of micropatterning and manipulation of cells for biomedical applications *Micromachines* **8** 347
[151] Kim J D, Choi J S, Kim B S, Chan Choi Y and Cho Y W 2010 Piezoelectric inkjet printing of polymers: stem cell patterning on polymer substrates *Polymer* **51** 2147–54
[152] Matsusaki M, Sakaue K, Kadowaki K and Akashi M 2013 Three-dimensional human tissue chips fabricated by rapid and automatic inkjet cell printing *Adv. Healthcare Mater.* **2** 534–9
[153] Sun Y N, Zhou X G and Yu Y D 2014 A novel picoliter droplet array for parallel real-time polymerase chain reaction based on double-inkjet printing *Lab Chip* **14** 3603–10
[154] Sun Y N, Song W H, Sun X H and Zhang S S 2018 Inkjet-printing patterned chip on sticky superhydrophobic surface for high-efficiency single-cell array trapping and real-time observation of cellular apoptosis *ACS Appl. Mater. Interfaces* **10** 31054–60
[155] Park J A, Yoon S, Kwon J, Now H, Kim Y K, Kim W J, Yoo J Y and Jung S 2017 Freeform micropatterning of living cells into cell culture medium using direct inkjet printing *Sci. Rep.* **7** 14610
[156] Bao B, Yoon S, Kwon J, Now H, Kim Y K, Kim W J, Yoo J Y and Jung S 2015 Fabrication of patterned concave microstructures by inkjet imprinting *Adv. Funct. Mater.* **25** 3286–94
[157] Carré A, Gastel J C and Shanahan M E R 1996 Viscoelastic effects in the spreading of liquids *Nature* **379** 432–4
[158] Park S J, Weon B M, Lee J S, Lee J, Kim J and Je J H 2014 Visualization of asymmetric wetting ridges on soft solids with x-ray microscopy *Nat. Commun.* **5** 4369
[159] Chung C, Shih K, R T, Chang C K, Lai C W and Wu B H 2011 Design and experiments of a short-mixing-length baffled microreactor and its application to microfluidic synthesis of nanoparticles *Chem. Eng. J.* **168** 790–8
[160] Ban M, Kogi Y and Hirose T 2019 Fabrication of arrayed microwells with wrinkle microstructure by ink-jet and diamond-like carbon thin film deposition process *Mater. Sci. Eng.* **249** 114422
[161] Scoutaris N, Alexander M R, Gellert P R and Roberts C J 2011 Inkjet printing as a novel medicine formulation technique *J. Control Release* **156** 179–85
[162] Daly R, Harrington T S, Martin G D and Hutchings I M 2015 Inkjet printing for pharmaceutics–a review of research and manufacturing *Int. J. Pharm.* **494** 554–67
[163] Maleki H and Bertola V 2020 Recent advances and prospects of inkjet printing in heterogeneous catalysis *Catal. Sci. Technol.* **10** 3140–59
[164] Uddin M J, Scoutaris N, Economidou S N, Giraud C, Chowdhry B Z, Donnelly R F and Douroumis D 2020 3D printed microneedles for anticancer therapy of skin tumours *Mater. Sci. Eng.* C **107** 110248
[165] Marizza P, Keller S S and Boisen A 2013 Inkjet printing as a technique for filling of micro-wells with biocompatible polymers *Microelectron. Eng.* **111** 391–5
[166] Jacot-Descombes L, Gullo M R, Cadarso V J and Brugger J 2012 Fabrication of epoxy spherical microstructures by controlled drop-on-demand inkjet printing *J. Micromech. Microeng.* **22** 074012
[167] Wang L, Luo Y, Liu Z Z, Feng X M and Lu B H 2018 Fabrication of microlens array with controllable high NA and tailored optical characteristics using confined ink-jetting *Appl. Surf. Sci.* **442** 417–22
[168] Yuan Y, Xu M, Wang X H, Lu H B and Qiu L Z 2021 Polyvinyl alcohol microlens array obtained by solvent evaporation from a confined droplet array *Appl. Opt.* **60** 10914–9
[169] Lauria I, Kramer M, Schröder T, Kant S, Hausmann A, Böke F, Leube R, Telle R and Fischer H 2016 Inkjet printed periodical micropatterns made of inert alumina ceramics induce contact guidance and stimulate osteogenic differentiation of mesenchymal stromal cells *Acta Biomater.* **44** 85–96
[170] Bietsch A, Zhang J Y, Hegner M, Lang H P and Gerber C 2004 Rapid functionalization of cantilever array sensors by inkjet printing *Nanotechnology* **15** 873–80
[171] Al-Milaji K N, Secondo R R, Ng T N, Kinsey N and Zhao H 2018 Interfacial self-assembly of colloidal nanoparticles in dual-droplet inkjet printing *Adv. Mater. Interfaces* **5** 1701561
[172] Wen L, Weaver J C and Lauder G V 2014 Biomimetic shark skin: design, fabrication and hydrodynamic function *J. Exp. Biol.* **217** 1656–66
[173] Wen L, Weaver J C, Thornycroft P J M and Lauder G V 2015 Hydrodynamic function of biomimetic shark skin: effect of denticle pattern and spacing *Bioinsp. Biomim.* **10** 066010
[174] Zhang L B, Wu J B, Hedhili M N, Yang X L and Wang P 2015 Inkjet printing for direct micropatterning of a superhydrophobic surface: toward biomimetic fog harvesting surfaces *J. Mater. Chem.* A **3** 2844–52
[175] Wu L, Dong Z C, Kuang M X, Li Y N, Li F Y, Jiang L and Song Y L 2015 Printing patterned fine 3D structures by manipulating the three phase contact line *Adv. Funct. Mater.* **25** 2237–42
[176] Nishimoto S *et al* 2009 TiO_2-based superhydrophobic–superhydrophilic patterns: fabrication via an ink-jet technique and application in offset printing *Appl. Surf. Sci.* **255** 6221–5
[177] Jiang J K, Bao B, Li M Z, Sun J Z, Zhang C, Li Y, Li F Y, Yao X and Song Y L 2016 Fabrication of transparent multilayer circuits by inkjet printing *Adv. Mater.* **28** 1420–6

[178] Sun J Z, Bao B, Jiang J K, He M, Zhang X Y and Song Y L 2016 Facile fabrication of a superhydrophilic–superhydrophobic patterned surface by inkjet printing a sacrificial layer on a superhydrophilic surface *RSC Adv.* **6** 31470–5

[179] Lee C, Kang B J and Oh J H 2016 High-resolution conductive patterns fabricated by inkjet printing and spin coating on wettability-controlled surfaces *Thin Solid Films* **616** 238–46

[180] Hou J, Li M Z and Song Y L 2018 Patterned colloidal photonic crystals *Angew. Chem., Int. Ed.* **57** 2544–53

[181] Kawata S, Sun H B, Tanaka T and Takada K 2001 Finer features for functional microdevices *Nature* **412** 697–8

[182] Zhang X, Jiang X N and Sun C 1999 Micro-stereolithography of polymeric and ceramic microstructures *Sens. Actuators* A **77** 149–56

[183] Sun C, Fang N, Wu D M and Zhang X 2005 Projection micro-stereolithography using digital micro-mirror dynamic mask *Sens. Actuators* A **121** 113–20

[184] Zheng X Y, Deotte J, Alonso M P, Farquar G R, Weisgraber T H, Gemberling S, Lee H, Fang N and Spadaccini C M 2012 Design and optimization of a light-emitting diode projection micro-stereolithography three-dimensional manufacturing system *Rev. Sci. Instrum.* **83** 125001

[185] Han D, Yang C, Fang N X and Lee H 2019 Rapid multi-material 3D printing with projection micro-stereolithography using dynamic fluidic control *Addit. Manuf.* **27** 606–15

[186] Kowsari K, Akbari S, Wang D, Fang N X and Ge Q 2018 High-efficiency high-resolution multimaterial fabrication for digital light processing-based three-dimensional printing *3D Print Addit. Manuf.* **5** 185–93

[187] Zhao Z, Tian X X and Song X Y 2020 Engineering materials with light: recent progress in digital light processing based 3D printing *J. Mater. Chem.* C **8** 13896–917

[188] Chivate A, Guo Z P and Zhou C 2022 Study of proximity effect in projection-based micro stereolithography process *Proc. 33rd Annual Int. Solid Freeform Fabrication Symp.—An Additive Manufacturing Conf.*

[189] Fouassier J P and Lalevée J 2012 *Photoinitiators for Polymer Synthesis: Scope, Reactivity, and Efficiency* (Wiley)

[190] Jenkins A D and Loening K L 1989 Nomenclature *Compr. Polym. Sci. Suppl.* **1** 13–54

[191] Lee J H, Prud'Homme R K and Aksay I A 2001 Cure depth in photopolymerization: experiments and theory *J. Mater. Res.* **16** 3536–44

[192] Jacobs P F 1992 *Rapid Prototyping & Manufacturing: Fundamentals of Stereolithography* (Society of Manufacturing Engineers)

[193] Kaur M and Srivastava A K 2002 Photopolymerization: a review *J. Macromol. Sci.* C **42** 481–512

[194] Hull C W 1986 Apparatus for production of three-dimensional objects by stereolithography *U.S. Patent* 4575330

[195] Wang X, Jiang M, Zhou Z W, Gou J H and Hui D 2017 3D printing of polymer matrix composites: a review and prospective *Composites* B **110** 442–58

[196] Zhu W *et al* 2017 Direct 3D bioprinting of prevascularized tissue constructs with complex microarchitecture *Biomaterials* **124** 106–15

[197] Soman P, Chung P H, Zhang A P and Chen S C 2013 Digital microfabrication of user-defined 3D microstructures in cell-laden hydrogels *Biotechnol. Bioeng* **110** 3038–47

[198] De Leon A C, Chen Q Y, Palaganas N B, Palaganas J O, Manapat J and Advincula R C 2016 High performance polymer nanocomposites for additive manufacturing applications *React. Funct. Polym.* **103** 141–55

[199] Zhou C and Chen Y 2009. Calibrating large-area mask projection stereolithography for its accuracy and resolution improvements *Proc. 2009 Int. Solid Freeform Fabrication Symp.* (University of Texas)

[200] Zhou C, Chen Y and Waltz R A 2009 Optimized mask image projection for solid freeform fabrication *ASME 2009 Int. Design Engineering Technical Conf. and Computers and Information in Engineering Conf.* (*San Diego, California, USA)*

[201] Zhou C and Chen Y 2012 Additive manufacturing based on optimized mask video projection for improved accuracy and resolution *J. Manuf. Process.* **14** 107–18

[202] Zhou C, Xu H and Chen Y 2021 Spatiotemporal projection-based additive manufacturing: a data-driven image planning method for subpixel shifting in a split second *Adv. Intell. Syst.* **3** 2100079

[203] Chivate A and Zhou C 2022. A modified schlieren system for in-situ voxel growth observation in projection-based stereolithography process *Proc.17th Int. Manufacturing Science and Engineering Conf.* (American Society of Mechanical Engineers)

[204] Chivate A and Zhou C 2023 Enhanced schlieren system for in situ observation of dynamic light–resin interactions in projection-based stereolithography process *J. Manuf. Sci. Eng.* **145** 081005

[205] Deng Q Y, Yang Y, Gao H T, Zhou Y, He Y and Hu S 2017 Fabrication of micro-optics elements with arbitrary surface profiles based on one-step maskless grayscale lithography *Micromachines* **8** 314

[206] Yuan C, Kowsari K, Panjwani S, Chen Z C, Wang D, Zhang B, Ng C J X, Alvarado P V Y and Ge Q 2019 Ultrafast three-dimensional printing of optically smooth microlens arrays by oscillation-assisted digital light processing *ACS Appl. Mater. Interfaces* **11** 40662–8

[207] Crow F C 1977 The aliasing problem in computer-generated shaded images *Commun. ACM* **20** 799–805

[208] Chivate A, Guo Z P and Zhou C 2024 Study of proximity effect in projection based micro vat photopolymerization process *Addit. Manuf.* **79** 103926

[209] Pucci K 2018 What is grayscale printing? (available at: https://imagexpert.com/what-is-grayscale-printing/)

[210] Park I B, Ha Y M, Kim M S, Kim H C and Lee S H 2012 Three-dimensional grayscale for improving surface quality in projection microstereolithography *Int. J. Precis. Eng. Manuf.* **13** 291–8

[211] Kristensson E, Ehn A and Berrocal E 2017 High dynamic spectroscopy using a digital micromirror device and periodic shadowing *Opt. Express* **25** 212–22

[212] Jariwala A S, Ding F, Boddapati A, Breedveld V, Grover M A, Henderson C L and Rosen D W 2011 Modeling effects of oxygen inhibition in mask-based stereolithography *Rapid Prototyp. J.* **17** 168–75

[213] Jariwala A S 2013 *Modeling and Process Planning for Exposure Controlled Projection Lithography* (Georgia Institute of Technology)

[214] Wu J T, Zhao Z A, Hamel C M, Mu X M, Kuang X, Guo Z Y and Qi H J 2018 Evolution of material properties during free radical photopolymerization *J. Mech. Phys. Solids* **112** 25–49

[215] Dabbagh S R, Sarabi M R, Rahbarghazi R, Sokullu E, Yetisen A K and Tasoglu S 2021 3D-printed microneedles in biomedical applications *iScience* **24** 102012

[216] Zheng X Y *et al* 2016 Multiscale metallic metamaterials *Nat. Mater.* **15** 1100–6

[217] Luongo A, Falster V, Doest M B, Ribo M M, Eiriksson E R, Pedersen D B and Frisvad J R 2020 Microstructure control in 3D printing with digital light processing *Comput. Graph. Forum* **39** 347–59

[218] Kowsari K, Zhang B, Panjwani S, Chen Z C, Hingorani H, Akbari S, Fang N X and Ge Q 2018 Photopolymer formulation to minimize feature size, surface roughness, and stair-stepping in digital light processing-based three-dimensional printing *Addit. Manuf.* **24** 627–38

[219] Shan Y J, Krishnakumar A, Qin Z H and Mao H C 2022 Reducing lateral stair-stepping defects in liquid crystal display-based vat photopolymerization by defocusing the image pattern *Addit. Manuf.* **52** 102653

[220] Montgomery S M, Demoly F, Zhou K and Qi H J 2023 Pixel-level grayscale manipulation to improve accuracy in digital light processing 3D printing *Adv. Funct. Mater.* **33** 2213252

[221] Janusziewicz R, Tumbleston J R, Quintanilla A L, Mecham S J and Desimone J M 2016 Layerless fabrication with continuous liquid interface production *Proc. Natl Acad. Sci. USA* **113** 11703–8

[222] Tumbleston J R *et al* 2015 Continuous liquid interface production of 3D objects *Science* **347** 1349–52

[223] Lee B J, Hsiao K, Lipkowitz G, Samuelsen T, Tate L and Desimone J M 2022 Characterization of a 30 μm pixel size CLIP-based 3D printer and its enhancement through dynamic printing optimization *Addit. Manuf.* **55** 102800

[224] Kochhar J S, Quek T C, Soon W J, Choi J, Zou S and Kang L F 2013 Effect of microneedle geometry and supporting substrate on microneedle array penetration into skin *J. Pharm. Sci.* **102** 4100–8

[225] Ligon S C, Liska R, Stampfl J, Gurr M and Mülhaupt R 2017 Polymers for 3D printing and customized additive manufacturing *Chem. Rev.* **117** 10212–90

[226] Johnson A R and Procopio A T 2019 Low cost additive manufacturing of microneedle masters *3D Print. Med.* **5** 2

[227] Johnson A R, Caudill C L, Tumbleston J R, Bloomquist C J, Moga K A, Ermoshkin A, Shirvanyants D, Mecham S J, Luft J C and Desimone J M 2016 Single-step fabrication of computationally designed microneedles by continuous liquid interface production *PLoS One* **11** e0162518

[228] El-Sayed N, Vaut L and Schneider M 2020 Customized fast-separable microneedles prepared with the aid of 3D printing for nanoparticle delivery *Eur. J. Pharm. Biopharm.* **154** 166–74

[229] Fang J-H, Liu C-H, Hsu R-S, Chen -Y-Y, Chiang W-H, Wang H-M D and Hu S-H 2020 Transdermal composite microneedle composed of mesoporous iron oxide nanoraspberry and PVA for androgenetic alopecia treatment *Polymers* **12** 1392

[230] Krieger K J, Bertollo N, Dangol M, Sheridan J T, Lowery M M and O'cearbhaill E D 2019 Simple and customizable method for fabrication of high-aspect ratio microneedle molds using low-cost 3D printing *Microsyst. Nanoeng.* **5** 42

[231] Lal Das A, Mukherjee R, Katiyer V, Kulkarni M, Ghatak A and Sharma A 2007 Generation of sub-micrometer-scale patterns by successive miniaturization using hydrogels *Adv. Mater.* **19** 1943–6

[232] Ochoa M, Zhou J, Rahimi R, Badwaik V, Thompson D and Ziaie B 2015 Rapid 3D-print-and-shrink fabrication of biodegradable microneedles with complex geometries *Proceedings of the 2015 Transducers-2015 18th Int. Conf. on Solid-State Sensors, Actuators and Microsystems (TRANSDUCERS)* (IEEE)

[233] Yao W, Li D D, Zhao Y L, Zhan Z K, Jin G Q, Liang H Y and Yang R H 2020 3D printed multi-functional hydrogel microneedles based on high-precision digital light processing *Micromachines* **11** 17

[234] Lim S H, Tiew W J, Zhang J Y, Ho P C L, Kachouie N N and Kang L F 2020 Geometrical optimisation of a personalised microneedle eye patch for transdermal delivery of anti-wrinkle small peptide *Biofabrication* **12** 035003

[235] Han D, Morde R S, Mariani S, La Mattina A A, Vignali E, Yang C, Barillaro G and Lee H 2020 4D printing of a bioinspired microneedle array with backward-facing barbs for enhanced tissue adhesion *Adv. Funct. Mater.* **30** 1909197

[236] Seong K Y, Seo M S, Hwang D Y, O'cearbhaill E D, Sreenan S, Karp J M and Yang S Y 2017 A self-adherent, bullet-shaped microneedle patch for controlled transdermal delivery of insulin *J. Control Release* **265** 48–56

[237] Khan A, Iqbal M J, Amin S, Bilal H, Bilquees H, Noor A, Mir B and Kaur M 2021 4D printing: the dawn of 'smart' drug delivery systems and biomedical applications *J. Drug Deliv. Ther.* **11** 131–7

[238] J L X *et al* 2021 Limpet tooth-inspired painless microneedles fabricated by magnetic field-assisted 3D printing *Adv. Funct. Mater.* **31** 2003725

[239] Chen X F, Liu W Z, Dong B Q, Lee J, Ware H O T, Zhang H F and Sun C 2018 High-speed 3D printing of millimeter-size customized aspheric imaging lenses with sub 7 nm surface roughness *Adv. Mater.* **30** 1705683

[240] Shao G B, Hai R H and Sun C 2020 3D printing customized optical lens in minutes *Adv. Opt. Mater.* **8** 1901646

[241] Kotz F, Arnold K, Bauer W, Schild D, Keller N, Sachsenheimer K, Nargang T M, Richter C, Helmer D and Rapp B E 2017 Three-dimensional printing of transparent fused silica glass *Nature* **544** 337–9

[242] Blachowicz T, Ehrmann G and Ehrmann A 2021 Optical elements from 3D printed polymers *e-Polymers* **21** 549–65

[243] Moussus M and Meier M 2021 A 3D-printed Arabidopsis thaliana root imaging platform *Lab Chip* **21** 2557–64

[244] Chen C, Rengarajan V, Kjar A and Huang Y 2021 A matrigel-free method to generate matured human cerebral organoids using 3D-Printed microwell arrays *Bioact. Mater* **6** 1130–9

[245] Luan Q Y, Becker J H, Macaraniag C, Massad M G, Zhou J, Shimamura T and Papautsky I 2022 Non-small cell lung carcinoma spheroid models in agarose microwells for drug response studies *Lab Chip* **22** 2364–75

[246] Tirado M, Kundu A, Tetard L and Rajaraman S 2020. Digital light processing (DLP) 3D printing of millimeter-scale high-aspect ratio (HAR) structures exceeding 100:1 *Proc. IEEE 33rd Int. Conf. on Micro Electro Mechanical Systems (MEMS)* (IEEE)

[247] Kaur G, Marmur A and Magdassi S 2020 Fabrication of superhydrophobic 3D objects by digital light processing *Addit. Manuf.* **36** 101669

[248] Ou J F, Cheng C Y, Zhou L, Dublon G and Ishii H 2015 Methods of 3D printing micro-pillar structures on surfaces *Proc. 28th Annual ACM Symp. on User Interface Software & Technology* (ACM)

[249] Lai H N, Gong B, Yin J and Qian J 2022 3D printing topographic cues for cell contact guidance: a review *Mater. Des.* **218** 110663

[250] Liu L Y, Liu S Y, Schelp M and Chen X F 2021 Rapid 3D printing of bioinspired hybrid structures for high-efficiency fog collection and water transportation *ACS Appl. Mater. Interfaces* **13** 29122–9

[251] Li X J, Yang Y, Liu L Y, Chen Y Y, Chu M, Sun H F, Shan W T and Chen Y 2020 3D-printed cactus-inspired spine structures for highly efficient water collection *Adv. Mater. Interfaces* **7** 1901752

[252] Ray S S, Dommati H, Wang J C, Lee H K, Park Y I, Park H, Kim I C, Chen S S and Kwon Y N 2021 Facile approach for designing a novel micropatterned antiwetting membrane by utilizing 3D printed molds for improved desalination performance *J. Membr. Sci.* **637** 119641

[253] Li C X, Wu L, Yu C L, Dong Z C and Jiang L 2017 Peristome-mimetic curved surface for spontaneous and directional separation of micro water-in-oil drops *Angew. Chem.* **129** 13811–6
[254] Yang Y, Li X J, Zheng X, Chen Z Y, Zhou Q F and Chen Y 2018 3D-printed biomimetic super-hydrophobic structure for microdroplet manipulation and oil/water separation *Adv. Mater.* **30** 1704912
[255] Kim D H, Kim S, Park S R, Fang N X and Cho Y T 2021 Shape-deformed mushroom-like reentrant structures for robust liquid-repellent surfaces *ACS Appl. Mater. Interfaces* **13** 33618–26
[256] Huang J D, Wang T J, Segura L J, Joshi G S, Sun H Y and Zhou C 2020. Spatiotemporal fusion network for the droplet behavior recognition in inkjet printing *Proc.15th Int. Manufacturing Science and Engineering Conf.* vol 84256 (American Society of Mechanical Engineers) p V001T01A038
[257] Wang S *et al* 2021 Machine-learning micropattern manufacturing *Nano Today* **38** 101152
[258] Samri M, Thiemecke J, Prinz E, Dahmen T, Hensel R and Arzt E 2022 Predicting the adhesion strength of micropatterned surfaces using supervised machine learning *Mater. Today* **53** 41–50
[259] Díaz Lantada A, Franco-Martínez F, Hengsbach S, Rupp F, Thelen R and Bade K 2020 Artificial intelligence aided design of microtextured surfaces: application to controlling wettability *Nanomaterials* **10** 2287